*universe*

MDPI

*Review*

# A Decade and a Half of Fast Radio Burst Observations

**Manisha Caleb [1,*] and Evan Keane [2,*]**

[1] Jodrell Bank Centre for Astrophysics, Department of Physics and Astronomy, The University of Manchester, Manchester M13 9PL, UK
[2] Centre for Astronomy, National University of Ireland Galway, University Road, H91 TK33 Galway, Ireland
* Correspondence: manisha.caleb@manchester.ac.uk (M.C.); evan.keane@gmail.com (E.K.)

**Abstract:** Fast radio bursts (FRBs) have a story which has been told and retold many times over the past few years as they have sparked excitement and controversy since their pioneering discovery in 2007. The FRB class encompasses a number of microsecond- to millisecond-duration pulses occurring at Galactic to cosmological distances with energies spanning about 8 orders of magnitude. While most FRBs have been observed as singular events, a small fraction of them have been observed to repeat over various timescales leading to an apparent dichotomy in the population. ∼50 unique progenitor theories have been proposed, but no consensus has emerged for their origin(s). However, with the discovery of an FRB-like pulse from the Galactic magnetar SGR J1935+2154, magnetar engine models are the current leading theory. Overall, FRB pulses exhibit unique characteristics allowing us to probe line-of-sight magnetic field strengths, inhomogeneities in the intergalactic/interstellar media, and plasma turbulence through an assortment of extragalactic and cosmological propagation effects. Consequently, they are formidable tools to study the Universe. This review follows the progress of the field between 2007 and 2020 and presents the science highlights of the radio observations.

**Keywords:** radio astronomy; fast radio burst; transient radio sources



**Citation:** Caleb, M.; Keane, E. A Decade and a Half of Fast Radio Burst Observations. *Universe* **2021**, *7*, 453. https://doi.org/10.3390/universe7110453

Academic Editors: Sergei B. Popov and Marta Burgay

Received: 29 October 2021
Accepted: 9 November 2021
Published: 20 November 2021



## 1. Foreword

The study of the dynamic and explosive radio Universe is an important and rapidly evolving branch of radio astronomy. Thus far, transient phenomena are known to occur on all timescales that have been investigated, from nanoseconds, e.g., the Crab nanoshot pulses; see [1] to years, e.g., supernovae and Gamma-ray bursts; see [2]. The X-ray, $\gamma$-ray and optical regions of the electromagnetic spectrum are the best explored with many space-based and ground-based instruments surveying the sky for serendipitous exotic events. Whilst recent advancements in radio astronomy instrumentation and signal processing have led to the benefits of high time resolution, this work has been hampered by the immense overheads required for signal processing and the need to combat radio frequency interference. Along with the historical dearth of appropriate wide-field survey instrumentation and systems, it has resulted in a large unexplored domain of potential transients. This review traces the evolution of one such new class of transients called fast radio bursts. The following sections attempt to encapsulate the excitement during the fledgling stage of the field, summarise the many advancements in our understanding of the associated science, and look at the now newly emerged sub-fields. Complementary to this article, a detailed review on the emission mechanisms can be found in Lyubarsky [3], a review on the multi-wavelength observations can be found in Nicastro et al. [4] and a review on the cosmological uses of FRBs can be found in Bhandari and Flynn [5].

## 2. The Beginnings of a Population

Intense bursts of electromagnetic radiation emanating from the distant Universe have altered our perception of the cosmos over the years, be it supernovae [6–8], pulsars,

e.g., [9,10], Gamma-ray bursts, e.g., [11,12] or the more recent kilonovae, e.g., [13]. One such burst of radio waves came to light in 2007 [14], and has heralded the identification of a new class of transients, the enigmatic "fast radio bursts" [15] or FRBs. As it happens the first FRB discoveries were likely made in the 1970s, by Linscott and Erkes [16]. Those signals, discovered using Arecibo, share many of the properties we would now identify with repeating FRB sources, but the inability to re-detect these sources in subsequent attempts [17] was, at the time, a roadblock for further work. For the prototypical 'Lorimer Burst' however this was not the case—this pulse was discovered in 2007 in an offset pointing of a survey of the Magellanic Clouds which had been conducted in 2001, in an endeavour to discover more of the then-emerging rotating radio transients [18].

The pulse was detected in 3 beams of the 13-beam Parkes multi-beam receiver [19] and was so bright ($S_\nu \gtrsim 30$ Jy) that it saturated one of the beams. This burst of radio emission was reminiscent of the signals discovered using Arecibo, and appeared to originate from beyond our Galactic neighbourhood. Therefore, it was nicknamed the 'Lorimer Burst' after its discoverer Duncan Lorimer [14]. The Lorimer burst (see Figure 1) displayed the classic dispersive sweep of propagation through cold, ionised plasma commonly seen in pulses from radio emitting neutron stars. By measuring the time delay of the signal across the observing frequency band, one can obtain the integrated column density of free electrons between the observer and the source through the dispersion measure (DM) given by,

$$\mathrm{DM} = \frac{1}{\mathcal{D}} \times \frac{\Delta t}{\Delta v^{-2}}, \tag{1}$$

where the scaling factor $\mathcal{D} = 4.1488064239(11)$ GHz$^2$ cm$^3$ pc$^{-1}$ ms [20], $\Delta t$ is the time delay across the observing band in seconds and $\Delta v$ is the observing bandwidth in GHz. The delay in arrival time in the observer's frame is $\Delta t = \Delta t'(1+z)$, where $\Delta t'$ is the rest-frame delay. Similarly, the observed frequencies in the observer's frame are $\nu_1 = \nu_1'/(1+z)$ and $\nu_2 = \nu_2'/(1+z)$ with $\nu_1'$ and $\nu_2'$ being the source rest-frame frequencies. Using these relations, the DM can be expressed as,

$$\mathrm{DM} = \int_0^z \frac{n_\mathrm{e}(z)}{(1+z)}\, dl, \tag{2}$$

where $n_\mathrm{e}(z)$ is the free electron density along the line of sight. As the path is cosmological in scale it makes sense to write this as $n_\mathrm{e}(z) = n_0(1+z)^3$, where the number density $n_0$ is related to the critical density of the Universe by the ionisation fraction $f_\mathrm{IGM}(z)$. The integral measure is $dl = c(dt/dz)dz$ and so contains another $(1+z)$ factor and the usual $E(z)$ cosmological scale factor [21]. Putting all the factors together and ignoring curvature and radiation terms in $E(z)$ we find [22]:

$$\mathrm{DM}_\mathrm{IGM}(z) = \frac{3cH_0\Omega_\mathrm{b}f_\mathrm{IGM}}{8\pi G m_\mathrm{p}} \times \int_0^z \frac{f_\mathrm{e}(z)\,(1+z)\,dz}{\sqrt{\Omega_m(1+z)^3+\Omega_\Lambda}}, \tag{3}$$

where $\Omega_b = 0.049$ is the present baryon density of the Universe [23], $f_\mathrm{IGM} = 0.83$ is the baryon mass fraction in the IGM [24,25], the matter density $\Omega_m = 0.308$, the vacuum density $\Omega_\Lambda = 0.6911$ and Hubble constant $H_0 = 67.74$ km s$^{-1}$ Mpc$^{-1}$ [23]. Just like in the case of Galactic pulsars [26], the DM can be thought of as a proxy for distance. The term $f_e(z)$ denotes the free electron number per baryon in the universe,

$$f_e(z) = \frac{3}{4}\chi_\mathrm{e,H}(z) + \frac{1}{8}\chi_\mathrm{e,He}(z) \tag{4}$$

with the terms $\chi_\mathrm{e,H}(z)$ and $\chi_\mathrm{e,He}(z)$ representing the ionization mass fractions of hydrogen and helium respectively.

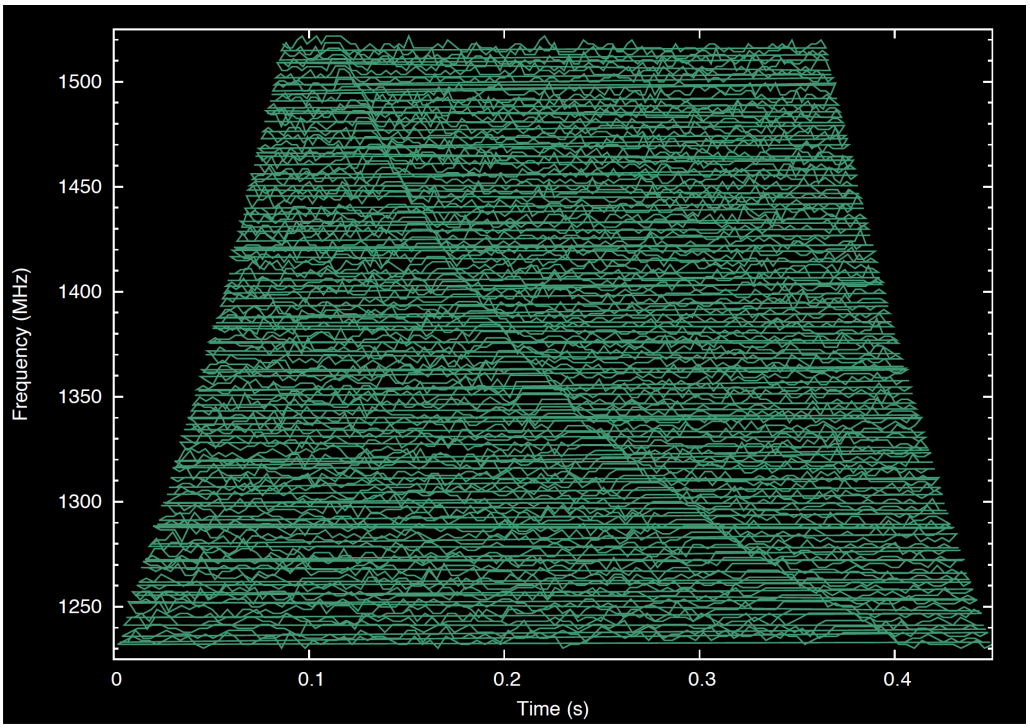


**Figure 1.** Time versus frequency plot aka the 'dynamic spectrum' of the main-beam detection (beam 6 of the Parkes multibeam receiver) of the 'Lorimer Burst'Lorimer et al. [14]. The frequency-dependent delay in arrival time of the signal due to the column density of free electrons in the propagation path, called dispersion measure, is shown by the quadratic sweep. The saturation of the receiver for this beam is evident by the flat-topped signal across thhe band. The flux density of this burst was ∼30 Jy. with a DM of 375 pc cm$^{-3}$. Only one eighth of this DM is accounted for, in this direction, by the Milky Way, suggesting an extragalactic origin.

The larger the value of DM, the more electrons the signal has interacted with in its path of propagation, and the further away the source producing the FRB is likely to be. The observed DM is typically a combination of various contributions along the line of sight (see Figure 2) given by,

$$\mathrm{DM}_{\mathrm{observed}}(z) = \mathrm{DM}_{\mathrm{MW}} + \mathrm{DM}_{\mathrm{IGM}}(z) + \frac{\mathrm{DM}_{\mathrm{host}} + \mathrm{DM}_{\mathrm{source}}}{1+z}, \quad (5)$$

where the various contributions are due to the interstellar medium (ISM) and halo of the Milky Way (at $z = 0$), the intergalactic medium (IGM) (along the entire path from $z = 0$ to $z = z_{\mathrm{FRB}}$), the ISM of the host galaxy and the environment in the immediate vicinity of the source (at $z = z_{\mathrm{FRB}}$). The electron density due to the ISM of our Galaxy can be accounted for as it has been well modeled using pulsars in the Galaxy [27,28]. The halo component contribution has been modelled to typically be between ∼30–50 pc cm$^{-3}$ [29,30], though some models suggest a wider range of values [31]. Due to the cosmological redshifting of frequency, we can see from Equations (2) and (3) that the combined contribution of the host galaxy and source is diluted by a factor of $(1 + z)$ to the Earth observer from the rest-frame observer [22,32] and is likely to be small. As a result, the $\mathrm{DM}_{\mathrm{IGM}}$ is the dominant contribution to the DM related to the FRB redshift ($z$) [22,33].

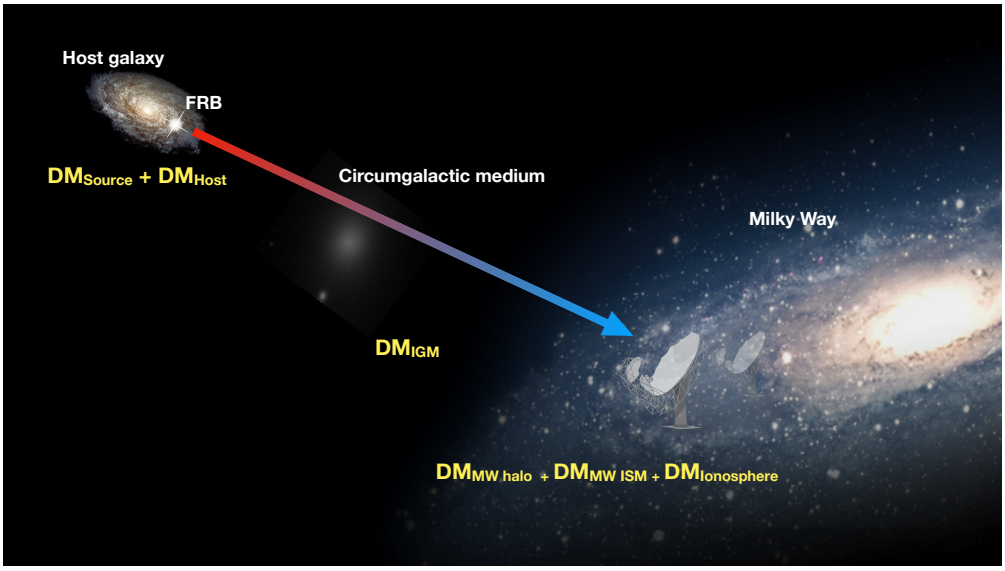


**Figure 2.** Cartoon of the various DM contributions along the path of propagation of the FRB signal and the corresponding distances.

In the absence of accurate measurements a rough redshift estimate for an FRB of a given DM can be obtained by using $z \lesssim \mathrm{DM_{IGM}}/[1000\,\mathrm{pc\,cm^{-3}}]$. There are quibbles [34,35] about the constant in this expression for an 'average' line of sight, but the existence of large-scale structures along different lines of sight may give lead to variations in the values of $\mathrm{DM_{IGM}}$ for the same redshift and can be upto 40% at $z\sim1$ [36]. Adopting this variation could affect the conversion factor [35]. Additionally, simulations suggest that observational biases for FRBs without redshift estimates may cause the *observed* linear DM-$z$ relation to be inverted such that the FRBs with the highest observed DMs may not be the most distant [37]. However, this is yet to be observationally proven with localised FRBs. The observed DM shows that the radio signal bears the imprint of the ionised material it traverses and as a result the radio data are a gold mine of information. They encode information about the progenitor source and its environment, the host galaxy, IGM, intracluster medium (ICM), the circumgalactic medium (CGM) and our own Milky Way. It can hold also a record of the magnetic field strength, the inhomogenities and also the turbulence encountered during its passage. Consequently, the signal is sensitive to a wide collection of extragalactic and cosmological propagation effects.

The discovery of the Lorimer burst took the media by storm and garnered immense public interest due to its enigmatic nature and short timescale. Despite astronomers trawling through archival data for multi-wavelength counterparts, and performing follow-up searches at radio wavelengths amounting to many tens of hours to detect repeat pulses, no concrete information regarding the origin was obtained [14]. With no more discoveries following the Lorimer burst, the excitement from 2007 gradually died down and for years the Lorimer burst was in a class of its own. Though the 'Keane burst' [38] was discovered in 2011 with similar observed characteristics to the Lorimer burst, its origin was argued to be Galactic due to likely sufficient diffuse ionised gas along the line of sight contributing towards the observed excess DM [38,39]. The Lorimer burst however has a measured DM of approximately 8 times the Galactic contribution which corresponds to a distance of 1.42 Gpc [14], thereby placing it without doubt outside the realms of the Milky Way. It wasn't then until 2013 when four more new bursts were discovered in the High Time Resolution Universe survey [40] using the Parkes radio telescope at 1.4 GHz [15], that the excitement was reignited in the fast transient community, and the class fast radio bursts was born. Similar to Gamma-ray Bursts (GRBs), the naming convention was defined to be FRB YYMMDD[1]. These new FRBs appeared to be fainter (e.g., $S_\nu\sim0.5$ Jy) and much farther away (e.g., $D_\mathrm{L}\sim3$ Gpc) than the Lorimer burst, which was perhaps an expected aspect of the 'winner's curse' [41]. Their larger distances made them much more intriguing, as the

farther away a source is, the greater its potential for use as a cosmological probe. Early occurrence rate estimates based on these discoveries suggested of order $\sim 10^4$ events sky$^{-1}$ day$^{-1}$ above a fluence[2] of 3 Jy ms [15].

Until 2013, all the FRBs had been discovered in archival data, which meant that the actual discovery of a burst could be years after the data were acquired. Fueled by the discoveries and results at Parkes, rapid advancements in real-time detection systems minimized the time lag between the occurrence of the burst and the time of detection. Astronomers had now entered the era of real time detections with the time lag being of order seconds instead of years. These real time detections were a milestone in FRB astronomy and hoped to provide answers to some of the burning questions. What was producing these energetic bursts? Did they occur in galaxies? Did they emit at other wavelengths? What could they tell us about the distant Universe? The questions and theories outnumbered the actual detections in the early days and thus began the worldwide race, to demystify and comprehend FRBs.

## 3. What Are FRBs?

FRBs are defined to be coherent radio pulses of typically millisecond duration, originating at extragalactic if not cosmological distances. Accounting for the Galactic contribution, the excess DMs of FRBs published to date place them well outside our Galaxy. On average, an FRB is observed to have a DM of $\sim$500 pc cm$^{-3}$, of which only about $\sim$50 pc cm$^{-3}$ is the Galactic contribution (assuming an ISM and halo contribution) as shown in Figure 3. Using the DM-$z$ scaling relation to obtain an upper limit on $z$, one can estimate the instantaneous or isotropic peak luminosity of an FRB given by,

$$L_{\rm FRB} = 4\pi D_{\rm L}^2 S_\nu, \tag{6}$$

where $D_{\rm L}$ is the luminosity distance in cm and $S_\nu$ is the specific peak flux in Jy or erg s$^{-1}$ cm$^{-2}$ Hz$^{-1}$ [35,42]. The isotropic energy of the FRB is expressed as,

$$E_{\rm FRB} = \frac{4\pi D_{\rm L}^2 \mathcal{F}_\nu \Delta\nu}{(1+z)}, \tag{7}$$

where $\mathcal{F}_\nu = S_\nu W$ is the the specific fluence in erg cm$^{-2}$ Hz$^{-1}$ or Jy ms, in which $W$ is the width in ms. FRB luminosities are in the range $10^{38} - 10^{46}$ erg s$^{-1}$ [43]. These immense energies required to produce these events at extragalactic/cosmological distances in order for them to be visible on Earth, along with their estimated high brightness temperatures, which are well in excess of thermal emission ($T_b > 10^{35}$ K), are what make them most tantalizing (see Figure 4). The typical observed widths of a few milliseconds (0.1–10 ms) combined with the light travel time indicate the characteristic length scale of the progenitor or engine producing the FRBs to be of the order 30–3000 kilometres, i.e., $R \sim c\Delta t$, where c is the speed of light and $t$ is the duration of the FRB. This is suggestive of compact object origins with most progenitor theories favouring neutron stars. The only stringent condition for the progenitor is that the frequency of emission must be greater than the plasma frequency of a non-magnetized plasma environment in order for the radio signal to propagate. Other observational properties that a model needs to account for are the millisecond durations, high isotropic energies, frequency structure and the high linear polarization in some cases. Synchrotron maser emission produced at the shock front between a wind nebula and the supernova remnant, as well as giant flares from within the magnetosphere are popular progenitor models.

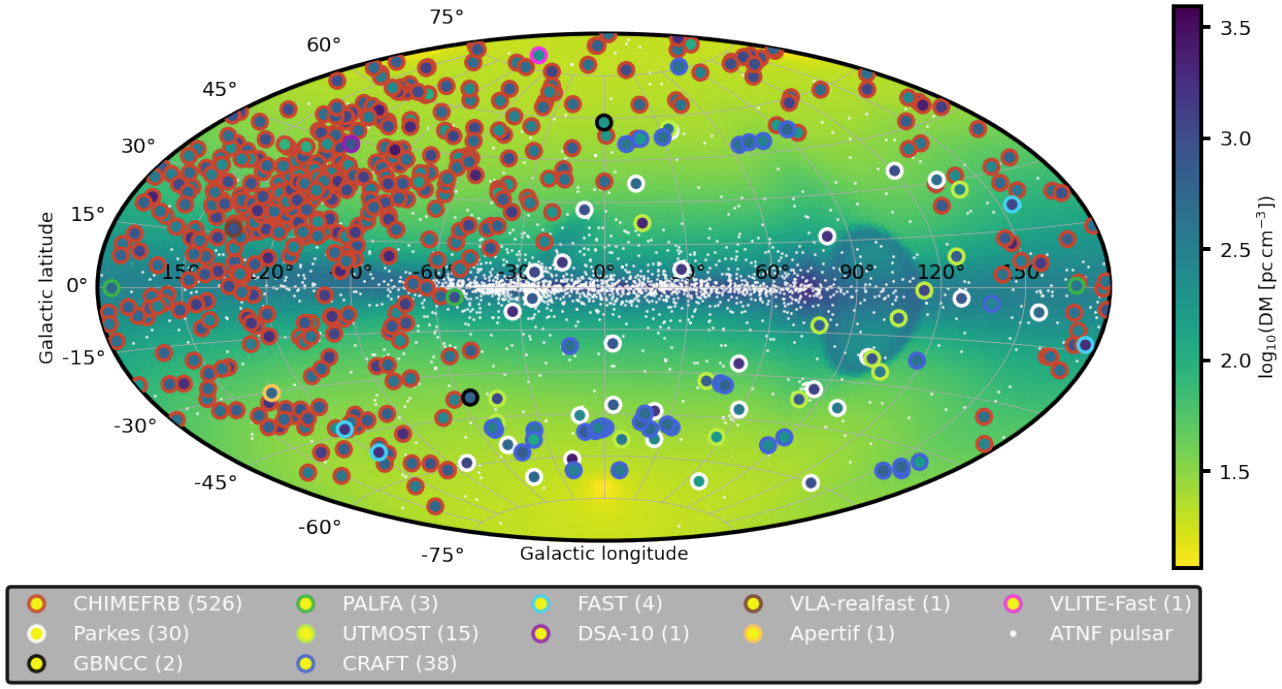


**Figure 3.** Aitoff projection of the all-sky distribution of FRBs detected by various telescopes across the world. The Galactic electron density distribution [28] is shown in the background. The FRBs are denoted by circles and follow the same color scale as the background. Any given FRB is observed to have a DM in excess of the Galactic contribution. The distribution of FRBs is almost isotropic. Any biases in the spatial distribution are likely due to differences in various survey depths and sky coverage. Credit: Laura Driessen.

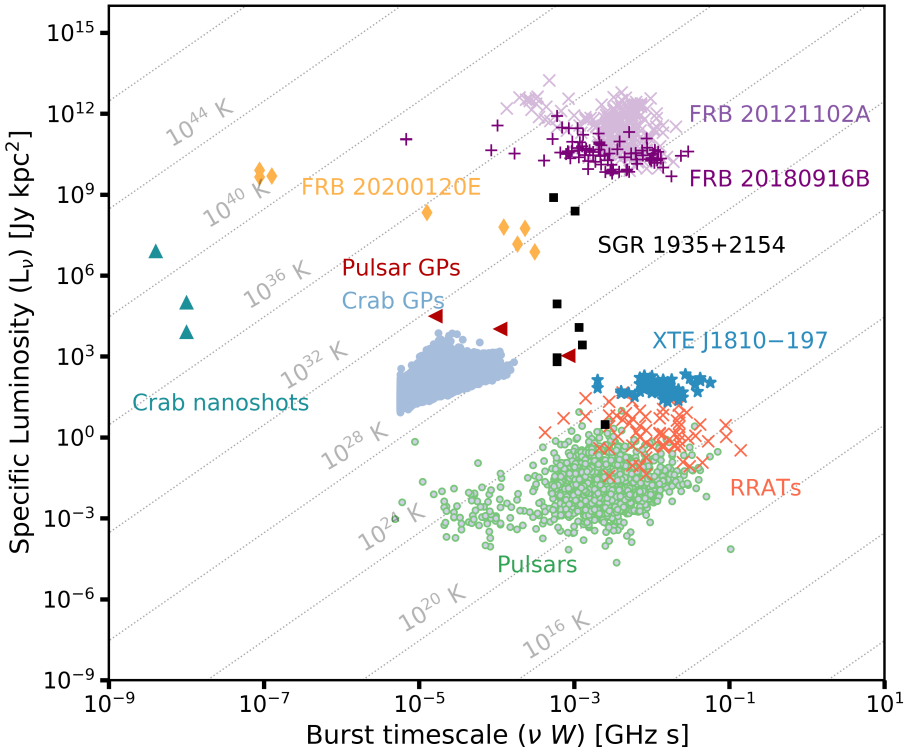


**Figure 4.** The ménagerie of short duration radio transients illustrating the various classes of events. The diagonal lines represent lines of constant brightness temperatures. For clarity of illustration, each pulsar and RRAT is represented by a single point, rather than their full brightness distribution.

Their $10^{12}$ times greater luminosities compared to pulsars and rotating radio transients (assuming beamed radiation) in Figure 4 suggests extreme neutron star manifestations as progenitors. Based on their observed characteristics, FRBs are the plausible outcomes of some of the most extreme processes in the Universe, such as the explosions and eruptions associated with the births and deaths of black holes or neutron stars. The matter and energies discharged from these explosions and eruptions are presumed to significantly effect galaxy evolution. These extraordinary attributes of FRBs provide a unique opportunity to probe fundamental physics and cosmology. A detailed review of the emission mechanisms and progenitors is presented in Zhang [44].

## 4. A Primer of FRB Science from 2007–2020

The field of FRB science had a head start in terms of lessons learned as GRB astronomy had provided many applicable examples from over the years. Arguably, the most important lesson to be learned from the study of GRBs is that identifying multi-wavelength counterparts and host galaxies was key to understanding their astrophysical nature. While 2013 saw the first real-time detection [45], 2014 began with the first discovery of an FRB at a observatory other than Parkes [46]. Following this, several more interesting discoveries such as the first polarized FRB [47] and the first detection at 800 MHz [48], ensued. It should be noted that until this point in time none of the known FRBs had been seen to repeat despite numerous follow-up attempts. However, the dawn of 2015 saw a groundbreaking discovery when the FRB 20121102A discovered at the Arecibo telescope in 2014, was found to repeat [49]. This allowed for several radio telescopes across the world with better angular resolution and higher sensitivity to target this FRB and subsequently localise it to a low-metallicity, star-forming, dwarf galaxy at a redshift $z = 0.19273(8)$ [50–52]. The localisation was a massive milestone in the field as it was concrete proof of cosmological origin. This was closely accompanied by the first interferometric detections of FRBs in 2016 [53].

With the development of new instrumentation and software, we have now reached a point where radical changes in the field occur on timescales of a few months and consequently, the field has increasingly gained momentum over the last decade. Especially in the last 3 or 4 years, we have seen an almost exponential rise in the number of detections and instantaneous localisations in the radio with new telescopes such as the Australian Square Kilometer Array Pathfinder (ASKAP) [54] and Canadian Hydrogen Intensity Mapping Experiment (CHIME) [55] coming online and turning into FRB detection machines. In spite of several discoveries over the last few years, the progenitors of FRBs remain unknown. Of the ∼600 published FRBs[3], ∼24 FRBs have been seen to repeat so far [56,57], suggesting that at least a subset have progenitors that can survive the energetic events causing them, e.g., [49]. It is presently unclear whether all FRBs repeat, and if repeating and apparently non-repeating FRBs form a unified population [58–60]. In addition to providing real-time, wide field-of-view instruments, the software and instrumentation developments have also resulted in the discovery of remarkable temporal structure on the microsecond level in pulses where high-time resolution data were available [61,62]. In comparison, typical blind detections at telescopes have millisecond durations due to telescope smearing time limitations. While FRBs are often defined as millisecond duration events with DMs in excess of the Galactic contribution (see Section 3), the discovery of microsecond-duration events, e.g., [62,63] as well as a possible FRB in our own Galaxy [56,64,65], calls into question the working observational definition of an FRB [66].

FRBs have been observed to emit at frequencies as low as 110 MHz [67] and as high as 8 GHz [68]. However, their emission outside this frequency range remains uncertain despite attempts to detect them beyond these frequencies [69,70]. The possible nature of the progenitors generating FRBs range from merging neutron stars and black holes, to axion stars [71] to newly born magnetars (see Platts et al. [72] for a complete list of theories). While they are just theories, recently the magnetar SGR J1935+2154 in our own Galaxy was observed to emit an FRB-like millisecond duration pulse by the CHIME [73,74]

and STARE2 telescopes [64], independently. The bursts has isotropic equivalent energies of $3 \times 10^{34}$ erg and $2.2 \times 10^{35}$ erg for assumed distances of 10 kpc and 9.5 kpc at the CHIME [74] and STARE2 [64] telescopes respectively. This burst was coincident with high-energy emission in the X-ray and Gamma-rays detected by several space-based telescopes, e.g., [75–78] resulting in the first contemporaneous multi-wavelength detection. This was a field-changing discovery as it was not only a step towards bridging the luminosity gap between Galactic sources (e.g., pulsars and rotating radio transients) and extragalactic FRBs (see Figure 4), but also evidence that at least a subset of FRBs could be generated by magnetars as it could be associated to the low-end of the FRB luminosity function. Regardless of their nature, localised FRBs with associated redshifts have a number of cosmological applications, e.g., [79,80]. Several theories predict FRBs to be extremely potent tools to study the nature of the magneto-ionic intergalactic medium [79,81], establish a chromatic scattering-redshift relation, possibly test Einstein's Equivalence Principle [82,83], measure the dark energy equation of state [84–86], examine baryonic feedback processes in galaxies [87], constrain the characteristic radial density profiles of CGM halos [88], and even detect and examine the elusive baryonic matter in the tenuous IGM [36]. Recently, the intersection of an FRB's sight-line with the circumgalactic medium of an intervening galaxy enabled stringent constraints on its halo gas density, magnetisation and turbulence [88]. Even more recently, a sample of arcsecond-localized FRBs was used to resolve astronomy's 'missing matter' problem by reporting a direct measurement of the baryon content of the Universe using FRB dispersion measures [89]. It has also been suggested that gravitationally lensed FRBs could independently provide constraints on two of the most important cosmological parameters: the Hubble constant [90,91] and cosmic curvature [86,92]. FRBs detectable with next generation telescopes like the Square Kilometer Array (SKA) and the Five-hundred-metre Aperture Spherical Telescope (FAST) at redshifts of 3 and above, are expected to carry the imprint of the epoch of helium reionization [22,93–95]. At the epoch of reionization we expect an observable variation in the steepness of the dispersion measure - redshift relation also known as the 'Macquart relation'. The detection and characterisation of this epoch may hold crucial information to aid in searches for the signature of the much sought after epoch of hydrogen reionization [96], at yet higher redshifts. FRBs have also been identified to improve galaxy-cluster kinetic Sunyaev-Zeldovich (kSZ) measurements of the growth rate and amplitude of cosmic density fluctuations [97], which is an important goal of the Dark Energy Spectroscopic Instrument (DESI) surveys. It is obvious that FRB science is highly complementary to existing multi-wavelength probes of cosmology. In fact, we have entered an era where these theories can already be tested and lead to high impact science results. With the potential of their uses as effective cosmological probes, and multi-wavelength detections of FRB-like pulses from a Galactic magnetar, it appears that FRBs have formed a bridge across cosmology, high-energy phenomena and stellar physics.

## 5. The FRB Population

With the increase in discoveries we have also seen an increase in the number of FRBs that go against our definition of a canonical FRB. While FRBs were initially defined as millisecond duration events with DMs in excess of the Galactic contribution, this is no longer the case with the detection of microsecond duration events and FRB-like pulses originating in our own Galaxy. Our understanding of the phenomenon is based on observations from various ground and space-based telescopes, and the inferences derived from them. Typically, at a radio telescope we measure the DM, signal-to-noise (S/N) ratio, pulse width, bandwidth of emission and spectral index. Furthermore, we also measure and quantify line-of-sight propagation effects such as scintillation, scattering, and Faraday rotation from polarization measurements. Additional information such as repeatability, periodicity and microstructure in the pulses in the case of high-time resolution detections can also be acquired. Overall, the FRBs discovered to date show a remarkable diversity of observed properties. The intrinsic properties such as polarization and intrinsic burst profile

shape provide us with information about the source itself, while the extrinsic properties such as the magnitude of Faraday rotation and multi-path propagation effects give us insight into the source's environment. The population as a whole refers to the thousand of events occurring across the sky every day, and the several hundreds of them detected at radio telescopes. See Table 1 for a list of telescopes currently undertaking FRB surveys and targeted searches. Understanding the population relies on combining the various observational properties to constrain theories. Astronomers have improved their understanding of the population using two popular strategies:

- Examine the population statistics and distributions of various observed and inferred properties using a large sample of bursts.
- Investigate specific properties of well-localised FRBs.

The results and science highlights of the two strategies are summarised in the the following sections.

**Table 1.** Summary of telescopes undertaking FRB surveys and targeted searches.

| Telescope | Centre Frequency (MHz) | Bandwidth (MHz) | No. of Polarizations | Reference |
|---|---|---|---|---|
| WSRT | 1370 | 300 | 2 | Connor et al. [98] |
| ASKAP Incoherent | 1272 | 336 | 2 | Bannister et al. [54] |
| ATCA | 5500 | 2000 | 2 | Petroff et al. [47] |
| | 7500 | 2000 | 2 | Petroff et al. [47] |
| CHIME | 600 | 400 | 2 | Bandura et al. [55] |
| DSA | 1400 | 220 | 2 | Ravi et al. [99] |
| DSN | 2250 | 115 | 2 | Majid et al. [100] |
| | 8360 | 450 | 2 | Majid et al. [100] |
| Effelsberg | 1360 | 300 | 2 | Hardy et al. [101] |
| | 6000 | 4000 | 2 | Hilmarsson et al. [102] |
| EVN | 1700 | 128 | 2 | Marcote et al. [52] |
| | 5000 | 128 | 2 | Marcote et al. [52] |
| FAST | 1250 | 500 | 2 | Luo et al. [103] |
| GBT | 350 | 100 | 2 | Chawla et al. [104] |
| GMRT | 650 | 200 | 2 | Marthi et al. [105] |
| LOFAR | 150 | 80 | 2 | Pastor-Marazuela et al. [106] |
| Lovell | 1400 | 336 | 2 | Rajwade et al. [107] |
| MeerKAT | 1284 | 856 | 2 | Jonas and MeerKAT Team [108] |
| | 816 | 544 | 2 | Jonas and MeerKAT Team [108] |
| MWA | 185 | 30 | 2 | Sokolowski et al. [69] |
| Northern Cross | 408 | 16 | 1 | Locatelli et al. [109] |
| Parkes | 2368 | 3300 | 2 | Hobbs et al. [110] |
| SRT | 328 | 64 | 2 | Prandoni et al. [111] |
| | 1400 | 500 | 2 | Prandoni et al. [111] |
| STARE2 | 1400 | 188 | 1 | Bochenek et al. [64] |
| UTMOST | 834 | 16 | 1 | Bailes et al. [112] |
| VLA | 1400 | 256 | 2 | Law et al. [113] |
| | 6000 | 2048 | 2 | Law et al. [113] |
| VLA (VLASS) | 3000 | 1500 | 2 | Law et al. [113] |

### *5.1. Frequency of Emission*

The first few FRBs that were discovered during the initial stages of the field were in pulsar surveys, which meant that most detections were at 1.4 GHz. However, once the detections grew in number at different telescope sites around the world, searches at higher and lower frequencies began, including coordinated campaigns across a wide range of wavelengths with 1.4 GHz driving the detection. Most wide-field, blind searches at lower frequencies have been unsuccessful at detecting FRBs, e.g., [114–116]. Though FRBs have now been detected from ∼110 MHz [67,106] all the way up to 8 GHZ [68], simultaneous detections across a wide and continuous frequency range have not been

observed yet. Also, emission beyond this frequency range is uncertain. This is primarily because the spectral behaviour of FRBs seen so far is very unusual, where the bursts are dominated by patches of bright emission with varying spectral indices across the bands [49,117]. For example, FRB 20121102A exhibits a wide range of spectral indices ($-10$ to $+14$) between consecutive pulses [49], and the Galactic FRB 200428 detected with the CHIME telescopes also shows a difference in spectral index between the two pulse components separated by $\sim$30 ms. Several targeted searches of repeaters as well as blind searches over hundreds of hours at low frequencies have been unsuccessful at discovering FRBs. This suggests spectral turnover due to free–free absorption, pulse broadening due to scattering, or a combination of the two for the observed non-detections. Additionally, it may also be that the intrinsic FRB coherent mechanism is not efficient at low frequencies. A coordinated campaign conducted with the Murchison Widefield Array (MWA) at $\sim$150 MHz to shadow FRBs detected by ASKAP at 1.4 GHz resulted in non-detections of seven ASKAP FRBs [69]. Similarly, simultaneous observations of FRB 20180916B over multiple epochs with WSRT at 1.4 GHz and LOFAR at 150 MHz resulted in 54 and 9 bursts respectively, all of which, are mutually exclusive detections in the two frequency bands [106]. Low frequency detections suggests that at least some FRBs reside in clean environments thereby allowing the propagation of the radio signal. How far low and how far high in frequency do FRBs emit is still to be determined.

### *5.2. Sky Distribution and Rates*

Figure 3 shows the all-sky distribution of FRBs as of June 2021. Early studies using a limited sample of bursts from the Parkes telescope concluded that the detection rate was greater at higher latitudes [118] with diffractive interstellar scintillation accounting for the deficit at low Galactic latitude [119]. This was explained by the fact that the scintillation bandwidth is much wider along high latitude sight lines, thereby boosting FRBs that might otherwise be rendered undetectable. More recent studies using a much larger sample of FRBs weakened the statistical significance of the latitude dependence [120]. Currently, assuming a cosmological distribution of FRBs, the all-sky rate is $\sim 10^5$ sky$^{-1}$ day$^{-1}$ above a fluence of 0.0146 Jy ms ($7\sigma$ for a 1 ms duration event) at 1.4 GHz [121]. The CHIME/FRB Catalog 1 rate at 600 MHz is $820 \pm 60^{+220}_{-200}$ sky$^{-1}$ day$^{-1}$ to a fluence limit of 5 Jy ms [122]. A cross-correlations of the CHIME/FRB sources with photometric galaxy surveys shows evidence for an order-one fraction of the CHIME FRBs being in the same dark matter halos as survey galaxies in this redshift range $0.3 \lesssim z \lesssim 0.5$ [123]. A more extensive study using hundreds of FRBs detected with better angular resolution may provide in the near future more information on the all sky distribution of FRBs and showcase any further clustering or concentrations in particular regions of the sky.

### *5.3. Repeatability and Periodicity*

The most obvious dichotomy in the population at the moment is seen in repetition. When it comes to repeatability in FRBs, the historical precedent is the case of soft gamma-ray repeaters (SGRs) versus cosmological catastrophic GRBs. However this might not quite be the case for FRBs, and whether all FRBs repeat is still an open question. It is possible that apparently non-repeating FRBs are produced by progenitors with long periods of quiescence, or the progenitors emit repeat bursts which are too faint to be detected by current radio telescopes. While it is impossible to prove something will never repeat, it is possible to place constraints. For many years FRB 20121102A was the only one observed to repeat. However, with the advent of CHIME, we have seen that repeaters may indeed be more common than initially thought [56,57]. Of the current sample of 24 repeating FRBs, most emit pulses sporadically and clustered in time, without a regular pattern. While no short timescale period has been detected between successive bursts for an FRB yet, a couple of prolific repeaters monitored over several years have resulted in the identification of long term periodicity, e.g., [107,124]. This discovery was unexpected as most FRB progenitor

model theories do not involve binary systems [72]. The three most well-studied repeating FRBs are discussed in detail below.

#### 5.3.1. FRB 20180916B

FRB 20180916B discovered at the CHIME telescope, is the first repeater for which a long term period was measured [124]. This FRB is observed to show repeats in bursts every $16.35 \pm 0.15$ days based on a Lomb-Scargle periodogram of the arrival times of 38 pulses over 2 years. All the bursts arrive in a five-day phase window, and 50 per cent of the bursts arrive in a 0.6-day phase window. High cadence observations over two years also show that repeat bursts don't appear every cycle [124]. Further follow-up observations of FRB 20180916B at frequencies higher than the operating frequency of CHIME resulted in bursts arriving at an earlier phase value compared to the low-frequency bursts. This indicates a possible correlation between frequency and phase, where high-frequency emission is suppressed at higher phase values [125]. More high-frequency observations over a variety of activity phases are required to test and prove this suggestion.

#### 5.3.2. FRB 20121102A

The discovery of periodic activity in FRB 20180916B was closely followed by the report of a long term period for the FRB 20121102A. Using a combination of the pulses in the literature and a high cadence monitoring campaign at the Jodrell Bank's Lovell telescope, Rajwade et al. [107] used a sample of 235 bursts detected over a time span of 7 years to estimate a period of $157 \pm 7$ days. Similar to FRB 20180916B, bursts were not detected during every active cycle. The period was independently confirmed by Cruces et al. [126] who estimated a value of $161 \pm 5$ days. No clear correlation between frequency and phase has yet been observed for this FRB. The wide range of long-term periods observed in FRBs 20180916B and 20121102A are reminiscent of the observed orbital periods of high mass X-ray binary systems of a neutron star in orbit with a massive O/B star [107,127,128]. Additionally, a precessing magnetar could also be responsible for the observed periodicity in the two FRBs [106,129,130]. Recently, Li et al. [131] report the detection of 1652 independent bursts of FRB 20121102A with no periodicity or quasi-periodicity between 1 ms and 1000 s.

#### 5.3.3. FRB 20171019A

The discovery of a periodicity in a repeating FRB source is an important clue to the nature of these objects. In both the cases mentioned above, the initial repeat bursts were discovered by the detection telescope. However, simulations have shown that FRBs can appear to be apparently non-repeating depending on the sensitivity of the telescope (e.g., [132]). That is to say, less sensitive telescopes would only detect the bright tail-end of the intrinsic energy distribution, which would therefore lead to bursts appearing as one-off events. An example of this is the FRB 20171019A discovered by the ASKAP telescope [117] in the lat50 survey, which comprised of observations of select high latitude fields. After the discovery, FRB 20171019A was followed up for over 500 h with a combination of the ASKAP and Parkes telescopes to search for repeat pulses [60], which resulted in no detections. However, $\sim$10 h of follow-up observations with the GBT in the UHF-band ($\sim$800 MHz) detected 2 repeat pulses $\sim$590 times fainter than the original detection at ASKAP [65]. Another repeat pulse was also independently observed by the CHIME telescope at 700 MHz [133]. It is possible that individual bursts have stochastic, patchy or modulated emission in different parts of the frequency band [65] (see Section 5.1). It is also possible that individual FRBs may repeat at much higher rates in parts of the spectrum that are not probed by these observations.

#### 5.3.4. To Repeat or Not to Repeat?

Several studies examine the existence of a single or multiple FRB populations. Most limits on repeatability thus far have been made using the original repeating FRB 20121102A

as a model. Palaniswamy et al. [58] consider a sample of one-off Parkes bursts and compare the limits on the wait-times and flux ratio between putative repeat bursts, with the measured values for FRB 20121102A. They suggest that it is possible that at least some FRBs are produced in catastrophic events so that they are intrinsically non-repeating FRBs. James [134] uses a method to limit the volumetric density of repeating FRBs based on the number (or lack) of repeating bursts identified in the ASKAP lat50 survey. He concludes that the FRB 20121102A is atypical of the population and cannot account for the 'single' bursts detected in the lat50 survey. The FRBs discovered in the survey could still however repeat at lower rates. Caleb et al. [132] present Monte Carlo simulations of a cosmological population of repeating FRB sources whose co-moving density follows the cosmic star formation rate history. Based on observations, they model all FRBs as repeating sources whose pulse arrival times follow either a Weibull [135] or Poisson distribution at various telescopes. They conclude that a single repeating population is still consistent with all observations, and that telescope sensitivity and the duration spent following up a source for repeat bursts are the main reasons for the observed dichotomy. Ravi [87] uses a sample of 12 nearby CHIME FRBs to compare the FRB volumetric rate with other astrophysical transients. He concludes that if FRBs are associated with compact objects produced through the standard astrophysical channels, the high FRB volumetric rate implies that the majority of FRB sources repeat. Ultimately, when nothing is known about the astrophysical nature of these sources, the absence of repeat bursts in some FRBs is suggestive of, but cannot prove, the existence of multiple origins.

### *5.4. Pulse Separations*

In addition to the long-term periodicity, short timescale separations or 'precursors' that precede the primary detection pulse have been observed. Precursors in pulses from FRB 20121102A have been detected by the Effelsberg telescope ($\sim$34 ms separation [101]) and more recently by the MeerKAT ($\sim$34 ms and $\sim$ 28 ms separations [136]) and Lovell telescopes ($\sim$17 ms separation; [107]). FRB 20121102A also exhibits 'postcursors', where a faint pulse follows a brighter primary pulse. These have been detected by the Green Bank [137] and Arecibo telescope [138] in 2016 with separations of $\sim$37 ms and $\sim$26 ms, respectively, and by the Effelsberg radio telescope in 2018 with a $\sim$38 ms separation [126]. Similar burst pairs are also reported by Gajjar et al. [68] and Gourdji et al. [138] with burst separations of $\sim$2 ms and $\sim$9 ms respectively. However, it is unclear whether these are single multi-peaked pulses or comprise two distinct bursts. Li et al. [131] present a bimodal waiting time distribution of 1652 independent bursts from FRB 20121102A, with a secondary peak centred at approximately 3.4 ms. They attribute this peak to the substructure of individual bursts, although some may be closely spaced, independent bursts. Pulse pairs have also been observed in the repeating FRB 20180916B [57,104,105,124] and the Galactic centre magnetar, FRB 200428 [64,74]. Other one-off FRBs that also exhibit pulse pairs are FRB 20190212A [56], FRB 20181112A [88,139], FRB 20190102C [61], FRB 20190611B [61], FRB 20181017C [63] and FRB 20170827A [140] with separation times ranging between $\sim$0.1–60 ms. The lack of a detectable short timescale period in these sources does not exclude a rotating object as a progenitor, as the detections of precursors and postcursors are suggestive of compact emission regions akin to a rotating object, in which multiple bursts are emitted during a single rotation.

### *5.5. Luminosity Function*

The ensemble or global luminosity function of FRBs refers to the number of bursts emitted with a certain luminosity across all FRBs, irrespective of whether they are repeaters. It gives the event rate per unit cosmic co-moving volume per unit luminosity. The shape of the luminosity function of FRBs is presently not well understood. While early analyses opted for power-law or normal distributions, more recent analyses assume a Schechter function, which has a power-law shape and a smooth exponential cut-off in the high luminosity end [43,141] given by,

$$\Phi(L)dL \propto \left(\frac{L}{L_*}\right)^{+\alpha} e^{-(\frac{L}{L_*})} dL. \quad (8)$$

Luo et al. [43] use Bayesian modelling and measure the FRB luminosity function of a sample of 46 FRBs. The data are found to be consistent with a power-law of index $\alpha \sim -1.8$ and upper cut-off luminosity $L_* \sim 3 \times 10^{44}$ erg s$^{-1}$. The lower cut-off in luminosity is estimated to be consistent with that of the Galactic FRB 200428 ($\sim 10^{38}$ erg s$^{-1}$) [44,142].

### *5.6. Emission Mechanisms and Progenitor Systems*

FRBs are recognised to be coherent radio emitters due to their short timescales and large brightness temperatures. In the case of progenitor systems, the central engine may act in isolation such as in the case of a precessing magnetar, or the activity may be kindled by an external plasma stream such as in the case of binaries. The coherent emission models are broadly classified into two categories: those involving FRBs produced within the magnetospheres of compact objects and those involving FRBs produced in relativistic shocks at distances beyond the magnetosphere. A detailed review of the emission mechanisms is presented in Lyubarsky [3]. In case of the magnetospheric model, the FRBs are generated via coherent curvature radiation by bunches [143,144] or magnetic reconnection [145]. While the emission mechanism has not been established conclusively, "bunches" with the necessary properties are theorised to exist in the magnetosphere. In the case of the shock model, FRBs are produced by synchrotron maser emission at ultra-relativistic magnetized shocks, such as those produced by flare ejecta from young magnetars [146]. While both types of models can elegantly explain most of the observed properties of FRBs, recent polarization and high-time resolution observations of a sample of FRBs appear to favour the magnetospheric origin model. Though high fractional linear polarization is predicted by both the synchrotron maser shock models and magnetospheric origin models, the observed constant polarization position angles in most repeaters is more naturally explained by the shock models. However, the diversity in polarization position angles observed in the repeating FRB 20180301A [103] is consistent with a magnetospheric origin of the radio emission, and disfavours the radiation models invoking relativistic shocks. Short timescale variations of $\sim$10 µs seen in FRB 20180916B [62] is also difficult to reconcile with the shock model without invoking a clumpy medium into which the shock front propagates. Additionally, the large energy budget required by the shock or synchrotron maser model makes a magnetorpheric origin more viable. Furthermore, periodic millisecond duration separations between components in pulses lasting a few seconds not only indicate a magnetorpheric origin, but also suggest the possible existence of a group of long/ultra-long duration/period FRBs. These separations may be explained by quasi-periodic oscillations predicted to originate from magneto-elastic axial (torsional) crustal eigenmodes originating close to the neutron star surface [147].

### *5.7. Volumetric Rates and Source Counts*

In addition to constraints on the luminosity function, observations and detections have also led to constraints on the occurrence rates and progenitors. The high all-sky rate of FRBs (see Section 5.2) relative to most observable radio transients places stringent constraints on their progenitors. The volumetric rate of FRBs based on the initial sample in Thornton et al. [15] is $\sim 2^4$ events Gpc$^{-3}$ yr$^{-1}$. The FRB rates can be compared with the estimated birth rates of potential progenitors under the assumption that the redshifts ascribed to the bursts are valid. The estimated rate is similar to the volumetric rate for SGRs $<2.5 \times 10^4$ events Gpc$^{-3}$ yr$^{-1}$ [148] and within an order of magnitude of the volumetric rate of core collapse (Type II) supernovae $\sim 2 \times 10^5$ events Gpc$^{-3}$ yr$^{-1}$ [149]. If FRBs are generated by one-off event such as binary neutron star mergers [150–152], they would only produce a very small fraction of special FRBs. However, if FRBs are generated by repeating sources such as magnetars [153] and pulsars [154] the sources producing the observed rate of FRBs can be far less abundant and easier to account for.

In a Euclidean Universe populated with objects of fixed luminosity (i.e., standard candles) and uniform number density, the number N detected above some flux limit $S$ varies as $N \propto S^{-\alpha}$, where $\alpha = -3/2$. Based on observations we know that FRBs have a broad luminosity distribution and are sufficiently distant that non-Euclidean effects become important. In a $\Lambda$CDM cosmology, $\alpha$ varies smoothly from a slope of $-3/2$ for the nearby universe, gradually becoming flatter as further distances are probed. Also, most surveys are "fluence incomplete" in the sense that events with the same fluence are easier to detect if they have narrower pulse widths (see Section 6 for details). Therefore, the cumulative source count distribution of FRBs is described as $N\,(> \mathcal{F}_{\rm min}) \propto \mathcal{F}_{\rm min}{}^{-\alpha}$, where $\mathcal{F}_{\rm min}$ is the minimum detectable fluence at a particular telescope. Various studies over the years employing different methods on samples from telescopes with different detection thresholds resulted in inconsistent values of source count distribution index ($-0.8 \geq \alpha \geq -2.6$ [155,156]). James et al. [37,157] jointly analysed a sample of Parkes and ASKAP FRBs modelling a stochastic DM-distance relation, FRB energy distribution function, as well as various selectiom effects simultaneously. Their best-fit model estimates a value of $\alpha = -1.5$ for a significant portion of the observed fluence range, changing to $-1.3$ for the fainter and more distant bursts detectable by Parkes. More recently, a large sample of FRBs subject to nearly identical biases detected by the CHIME telescope was used to infer a value of $\alpha = -1.40 \pm 0.11(\text{stat.})^{+0.06}_{-0.09}(\text{sys.})$ [122], consistent with a non-evolving Euclidean population. The difference in the median DM values observed in the Parkes ($\sim$900 pc cm$^{-3}$) and CHIME ($\sim$500 pc cm$^{-3}$) sample of FRBs makes it plausible that the Parkes FRBs are more distant and subject to cosmological and/or evolutionary effects thereby flattening the distribution [122].

### *5.8. Pulse Morphology*

The FRB pulses observed to date show remarkable spectral and temporal variations and structure. The unusual spectral behaviour of FRBs seen so far is best showcased in high time resolution observations. FRBs are seen to exhibit scattering, scintillation, microstruture and frequency down-drifting (see Figure 5). These attributes which are detailed below, are key to understanding the underlying emission mechanism and any turbulence and inhomogenieties in the intervening medium.

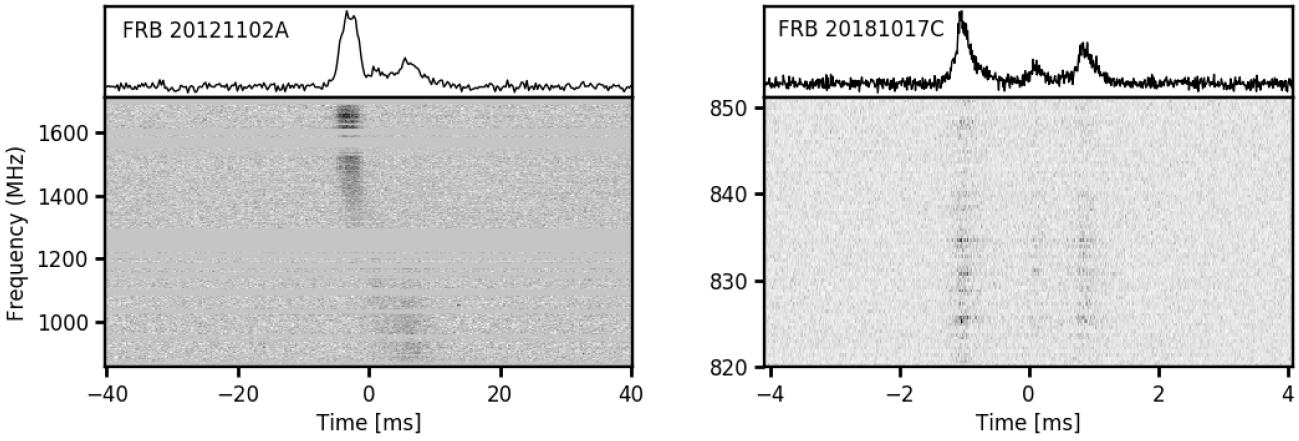


**Figure 5.** Dynamic spectra of FRBs 20121102A and 20181017C detected at the MeerKAT and UTMOST telescopes respectively. The top panel in each pulse shows the frequency-averaged pulse profile. The data are uncalibrated, and the flux densities are in arbitrary units. *Left panel*: The single pulse from FRB 20121102A has been dedispersed to the structure maximising DM which reveals downward frequency drifting in three distinct features. The data have a time resolution of 306.24 µs. *Right panel*: The single three-peaked pulse from FRB 20181017C has a time resolution of 10 µs as voltage data was recorded. The three peaks have consistent scattering timescales and pulse widths and show frequency striations of a few 100 kHz due to scintillation.

5.8.1. Scattering

Scattering is caused by multi-path propagation through cold-ionised plasma as evidenced by the exponential-like scattering tail on the trailing edge of the pulse [158,159]. A point source therefore appears broadened in the image plane. A thin screen model of irregularities of various scales can account for this observed pulse width broadening. This decay time of the exponential or scatter timescale is greatly dependent on the observing frequency, expressed as,

$$\tau_s \propto \nu^{-4}, \quad (9)$$

with greater scattering expected at lower frequencies. Most FRBs have been detected at high Galactic latitudes where the scattering due to the ISM of the Galaxy is weak, implying that the scattering screen lies beyond the Milky Way. It is however unclear whether the screens lie closer to the local environments of FRBs, or in the IGM and the CGM of intervening galaxies in the absence of host galaxy measurements. Qiu et al. [160] use Bayesian inference to analyse a sample of 33 FRBs discovered by the ASKAP telescope and find evidence for scattering broadening in 5 of them. One of the FRBs with the best evidence of scattering is FRB 20180110A with a measured index of $-3.7 \pm 0.9$. No strong evidence of correlation between DM and scatter broadening was observed in the sample used by Qiu et al. [160], similar to what has been observed for pulsars in our Galaxy [161]. Using a sample of CHIME FRBs, Chawla et al. [162] cannot rule out a model of FRBs for which scattering originates in both in the local environment and in intervening galaxies. Additionally, they infer that the circumburst media of FRBs must have more extreme properties than those of typical Galactic plane environment.

5.8.2. Scintillation

Similar to pulsars, FRBs show short-term variations in brightness or 'scintles' as a function of frequency, attributed to the constructive and destructive interference caused by the multi-path propagation of the signal through turbulent, ionised electron density concentrations. Scintillation in the strong scattering regime (large variations in phase over the Fresnel scale) is dominated by two distinct branches: diffractive (scales of $\sim 10^6$–$10^8$ m) and refractive (scales of $\sim 10^{10}$–$10^{12}$ m). This spectral modulation is seen as the densities in the ISM move by the Earth, and the timescale of the intensity of the fluctuations depend on the relative velocities of the densities in the intervening medium, the FRB, and the Earth. Interference can occur only if the condition of $2\pi\Delta\nu\tau_s \sim 1$ is satisfied, in which $\Delta\nu$ is the 'decorrelation bandwidth' or 'scintillation bandwidth' and is the typical bandwidth of correlated intensity fluctuations for a source. This shows that the the scintillation bandwidth is related to the scattering time and scales as $\Delta\nu \sim 1/\tau_s \propto \nu^4$. FRBs 20121102A [163], 20150807A [164], 20170827A [140] and 20181017C [63] in particular show distinctive scintles in their spectra. FRB 20150807A's scintillation is possibly due to weak turbulence in the plasma in the IGM or host galaxy [164]. FRB 20170827A exhibits both broadband scintillation accounted for by the turbulence in the ISM of the Milky Way, as well as narrower striations of a few frequency channels wide spanning ∼150 kHz suggestive of a screen along the path of propagation [140]. The origin of the few 100 kHz striations seen in FRB 20181017C are less constrained, with possibilities including turbulence in the Galactic ISM, IGM, the source or the ISM of the host galaxy [63]. Pulses from FRB 20121102A in the L-, S- and X-bands exhibit narrow-band fluctuations of burst intensity consistent with scintillation from the ISM of the Milky Way at the observed low Galactic latitude of the FRB [100,163].

Interstellar scintillation is also expected to amplify the emission from some FRBs such that pulses which would typically be too weak to be detected are pushed above the threshold of detectability [119]. However, the typical scintillation bandwidths at the Galactic positions of FRBs are much smaller than the wide observing bandwidths possibly resulting in no amplification of the signal (see Section 5.2). Therefore it is unlikely that scintillation plays a major role in the detectability of FRBs.

#### 5.8.3. Microstructure

The durations of transient events discovered in searches at radio telescopes are sometimes limited by the instrumental sampling and smearing time, which lead to the broadening of a pulse. The true intrinsic pulse width and shape are recoverable through coherent dedispersion of the raw voltage data from the telescope. An example of this is the real-time detection of FRB 20181112A discovered at the ASKAP telescope operating with time and frequency resolutions of $\sim$1 ms and $\sim$1 MHz respectively. The processing of the recorded high-time resolution data allowed Cho et al. [139] to probe emission timescales down to microseconds. While the real-time detection was a single peak with a pulse width of $2.1 \pm 0.2$ ms, coherent dedispersion resulted in the identification of four-microsecond duration pulses under the main burst envelope. Similarly, FRB 20181017C discovered at UTMOST as a single-peaked millisecond duration event in the real-time detection system was resolved into 3 distinct components in the coherently dedispersed high-time resolution voltage data [63] (see Figure 5). Neither FRB 20181017C nor FRB 20181112A show evidence for phase-coherence between the pulse component supporting plasma lensing or periodicity in the arrival times.

Microstructure in pulses represents the shortest time scale fluctuations in the total intensity measured so far. These timescales constrain the instantaneous size of the emitting region and consequently, the emission mechanism. Notable FRBs that show these features are FRB 20121102A, 20170827A, 20180916B and 20181112A. In the case of FRB 20181112A, the observed widths are limited by the scattering timescale. FRB 20121102A showed a 30 µs wide burst component at 4.5 GHz [165]. A study of voltage data recorded during observations of FRB 20180916B shows bursts with structure as narrow as 3–4 µs, and spanning close to 3 orders of magnitude up to $\sim$2 ms within individual bursts [62]. This implies an emission region of $\sim$1 km [62]. On average, the observations of microstructure indicate emission regions of the order of a few hundred km (see Section 1). This suggests a magnetospheric origin model (also referred to as the pulsar-like emission model) in which the radio burst occurs close to, or within the magnetosphere of the central engine, compared to the shock model in which relativistic shocks are generated by an explosive energy release from the central engine at larger distances. In the case of an FRB originating at a shock front rather than the magnetosphere of the progenitor, a relatively small area of the shock front is expected to contribute to the emission.

#### 5.8.4. Frequency Drifting a.k.a the Sad-Trombone Effect

An interesting property of FRBs is the recently discovered complex time–frequency structures which include sub-bursts that are band-limited, e.g., [106,136,163]. Until recently, all FRB pulses were dedispersed to the DM that maximises S/N, which may lead to any burst structure being unresolved. When dedispersed to the structure-maximising DM, these pulses can exhibit multiple sub-burst components under the same emission envelope. They have also revealed a downward drift of the sub-bursts in frequency such that the lower frequencies arrive at later times within the burst envelope. These downward drifts (also referred to as the 'sad-trombone effect') are more common in FRBs which repeat and is likely a combination of the unknown emission mechanism and line-of-sight propagation effects. The drifting has been explained by the magnetar models in which a decelerating shock wave causes a temporal decrease in the peak frequency resulting in the observed drift [146]. Within the framework of magnetospheric emission, the drifting is explained either through transient pulsar-like sparking from the inner gap region of a slowly rotating neutron star, or through externally-triggered magnetosphere reconfiguration [166]. Plasma lensing (see Section 5.8.5) has also been proposed as a likely cause of the frequency drifting due to a source induced bow shock in a dense medium or filaments in a supernova remnant. Intriguingly, the downward drift is larger towards higher frequencies, e.g., [104,106,163,167]. The two most well-studied FRBs across a wide range of frequencies, which also exhibit downward drifting sub-bursts are FRBs 20121102A and 20180916B. Even though they reside in markedly different host galaxies and local environments (see

Sections 5.9 and 5.11) it appears that there might exist a shared sub-burst drift law among repeaters [168]. A larger sample of repeaters is required to examine if these features are indeed common among all repeating FRBs or at least a significant subclass of them. If proven to be a common property, it will likely offer significant clues to the FRB emission mechanism. It appears that while the downward drifting structure is more common in repeaters than non-repeaters, several repeat bursts do indeed occur without significant drifting sub-structure [56,57]. Therefore, the lack of drifting structure in a burst is presently insufficient to classify the FRB as a non-repeater. Additionally, downward-drifting structure may be unresolved in coarse time resolution data. Coherent dedispersion and analysis of voltage data of repeater and one-off bursts is important to understanding whether the presence of downward-drifting structure is predictive of repetition.

#### 5.8.5. Plasma Lensing

Plasma lensing caused by one dimensional over- or under-dense Gaussian lenses in the proximity of the source of the FRB, or farther out in the host galaxy has been considered as a possible cause of the frequency drifts seen in FRBs, e.g., [169]. The focal length of a lens must be less than the distance to the observer from the lens for caustics to form. However, the predominance of downward frequency drifts in repeating FRBs is puzzling. Should lensing occur, one would expect to observe both downward and upward frequency drift: as the viewing geometry changes, the drift rate is expected to change rate and signs. Potential upward drifting behaviour has been reported before in repeating (periodic) FRBs 20121102A [170] and 20180916B [67], and in the apparently one-off FRB 20190611B [61]. However, when pulses consist of two sub-bursts, it is unclear whether the pulses are independent or occur within the same burst envelope, thereby providing only tenuous evidence.

### *5.9. Polarization*

Polarization is typically used to probe the presence of magnetic fields. In pulsar or transient search modes, only data containing the total intensity information of a source is typically recorded as full Stokes polarization data products are larger in size and not feasible for storage on a regular basis. Additionally, some telescopes do not possess the capacity to measure polarization. A linearly polarized wave is the superposition of left and right circularly polarised waves. On propagation through a magnetised plasma, the right and left circularly polarized components are phase shifted by different amounts or equivalently the plane of the linearly polarised component is rotated. This birefringent effect is called Faraday rotation. The angle between the plane of linear polarization and the plane of reference is called the polarization position angle and the amount of rotation undergone is quantified by the rotation measure (RM) given by,

$$\mathrm{RM} = \frac{\mathrm{e}^3}{2\pi m_\mathrm{e}^2 c^4} \int_0^d n_\mathrm{e} B_{||} dl \tag{10}$$

where $d$ is the distance to the source, $n_\mathrm{e}$ is the electron density along the line of sight (LOS), $B_{||}$ is the magnetic field parallel to the LOS, and $dl$ is the elemental vector towards the observer along the LOS. The sign of the RM depends on whether the field direction is oriented towards (negative) or away (positive) from the observer. The effects of Faraday rotation are strong in the radio part of the electromagnetic spectrum and are observable in any plasma irrespective of whether or not those atoms/molecules have magnetically susceptible energy levels. This indicates that we can ignore interstellar extinction and thus probe magnetic fields out to cosmological distances. Polarization information is crucial to discerning the emission physics behind the sources, and RMs can offer significant clues to the origins of FRBs. Faraday rotation can manifest itself not only as a change in the polarisation angle with frequency but also as a change in the polarised flux density (depolarization) with frequency. The raw polarization measured by a radio telescope could differ from the true polarization of the source due to a number of effects such as

the propagation of the wave through the medium between the source and telescope, and various instrumental non-idealities. The ultimate aim is to correct for these effects in order to derive the true source polarization properties.

In the case of extragalactic FRBs, the observed total RMs would be a combination of different contributions along the lines-of-sight given by,

$$\mathrm{RM_{obs}} = \mathrm{RM_{Galactic}} + \mathrm{RM_{iono}} + \mathrm{RM_{IGM}}(z) + \mathrm{RM_{host}}(z) + \mathrm{RM_{source}}(z). \quad (11)$$

$\mathrm{RM_{Galactic}}$ is the Galactic component assumed to typically vary with Galactic latitude and longitude and includes the local universe RM contributions, $\mathrm{RM_{iono}}$ is the RM due to the Earth's ionosphere, $\mathrm{RM_{IGM}}$ is the contribution from the intergalactic medium in the form of galaxies or filaments of cosmological large-scale structures along the LOS, $\mathrm{RM_{host}}$ is the RM due to anomalous regions in a host galaxy, and $\mathrm{RM_{source}}$ is the intrinsic component from magnetized plasma associated with the progenitor source and its immediate environment. In the case of a source at cosmological distances, the RM along the line of sight after accounting for the contributions from $\mathrm{RM_{Galactic}}$ and $\mathrm{RM_{iono}}$ will be reduced by a factor of $(1+z)^2$ as,

$$\mathrm{RM}(z) = \frac{\mathrm{e}^3}{2\pi m_\mathrm{e}^2 c^4} \int \frac{n_\mathrm{e}(z) B_{||}(z)}{(1+z)^2} \frac{dl}{dz}, \quad (12)$$

due to the redshifting of the observed frequencies. Based on the RM and DM, the average magnetic field along the LOS weighted by electron density can be estimated as,

$$\langle B_{||} \rangle \approx \left(\frac{\mathrm{RM}}{\mathrm{rad\,m^{-2}}}\right) \left(\frac{\mathrm{DM}}{\mathrm{pc\,cm^{-3}}}\right)^{-1} \mathrm{G}. \quad (13)$$

The measured magnetic field is typically a lower limit due to possible line of sight magnetic field reversals caused by intervening components-like filaments or galaxies. Of the ∼600 published FRBs, only 20 have measured RMs. This sample of 20 contains FRBs which are highly linearly and circularly polarised. FRBs 20140514A and 20160102A are notable for their significant circular polarization fractions in addition to their high linear fractions (see Table 2). Conversion of linear into circular polarization through Faraday conversion in the intervening media has been proposed as a cause for the observed circular polarization fractions [171,172]. FRBs with observed RMs in excess of the Galactic contribution suggest an ordered magnetic field local to the host galaxy or progenitor. Conversely, in the FRBs where the observed RM is almost similar to the Galactic contribution there exists no ordered magnetic field local to the host or progenitor. No coherent picture has yet emerged from the relatively small sample of available RMs.

Figure 6 shows FRBs and Galactic pulsars as a function of RM and DM. The shaded regions enclose the ranges of potential RMs (∼few to $\sim 10^5$) and DMs for various progenitor models. The repeating FRB 20121102A is observed to have the highest measured RM by far, comparable to that of the Galactic centre magnetar J1745−2900. A decades-old neutron star embedded within a still-compact supernova remnant, or a neutron star near a massive black hole and its accretion torus have been proposed to explain the high RM [50,165,173]. On the contrary, non-repeating FRBs have RMs smaller by orders of magnitude and comparable to those of Galactic pulsars indicating that they are not associated with galactic nuclei [174]. However, the proximity of some repeating FRBs to non-repeating FRBs and pulsars suggests that repeating FRBs may in fact reside in various different environments. Some progenitor models expect the peak burst rate to decrease with source age [146,175], which suggests that these sources may be older compared to FRB 20121102A. This is supported by the observed erratic, short-term RM variations of $\sim 10^3$ rad m$^{-2}$ week$^{-1}$ and overall decrease of RM from $1.4 \times 10^5$ rad m$^{-2}$ to $6.7 \times 10^4$ rad m$^{-2}$ in FRB 20121102A over ∼2.6 years [102]. If all FRBs are repeaters belonging to a single population, FRB 20121102A might be a particularly young and active specimen at a different evolutionary phase compared to the others. Interestingly, the two best-characterised repeating FRBs 20121102A and 20180916B, which have also been localised to host galaxies (see Section 5.11),

exhibit similar polarimetric properties. They show ∼100% linear polarization and 0% circular polarization with a roughly flat polarization angle during and between bursts [62,106,163,165]. The similarity in the spectro-temporal polarimetric properties of these bursts suggests that they have the same progenitor type and emission mechanism.

**Table 2.** Summary of the polarization properties measured in the FRB sample available so far. The second and third columns list the observed fractional linear and circular polarization, respectively.

| FRB Name | $L$(%) | $V$(%) | Total RM (rad m$^{-2}$) | Galactic RM (rad m$^{-2}$) | Reference |
|---|---|---|---|---|---|
| 20110523A | $44 \pm 3$ | $23 \pm 30$ | $-186.1 \pm 1.4$ | $18 \pm 13$ | Masui et al. [48] |
| 20121102A | 100 | – | $67030 \pm 90$ | $-25 \pm 80$ | Hilmarsson et al. [102] |
| 20140514A | <10 | $21 \pm 7$ | – | – | Petroff et al. [47] |
| 20150215A | $43 \pm 5$ | $3 \pm 1$ | $-9 <$ RM $< 12$ | – | Petroff et al. [176] |
| 20150418A | $8.5 \pm 1.5$ | – | $36 \pm 52$ | – | Keane et al. [177] |
| 20150807A | $80 \pm 1$ | – | $12.0 \pm 7$ | 13.3 | Ravi et al. [164] |
| 20151230A | $35 \pm 13$ | $6 \pm 11$ | – | – | Caleb et al. [178] |
| 20160102A | $84 \pm 15$ | $30 \pm 11$ | $-220.6 \pm 6.4$ | 24.6 | Caleb et al. [178] |
| 20171209A | 100 | – | $121.6 \pm 4.2$ | | Osłowski et al. [179] |
| 20180301A | ≥70 | ≤3 | 517 | $72 \pm 8$ | Luo et al. [43] |
| 20180309A | $45 \pm 0.06$ | $24.33 \pm 0.05$ | $\|$RM$\|$ < 150 | – | Osłowski et al. [179] |
| 20180311A | $75 \pm 3$ | $4.8 \pm 7.3$ | $4.8 \pm 7.3$ | – | Osłowski et al. [179] |
| 20180714A | $91 \pm 3$ | $5 \pm 2$ | $-25.9 \pm 5.9$ | – | Osłowski et al. [179] |
| 20180916B | ≥80 | ≤15 | $-104 \pm 20$ | – | Nimmo et al. [62] |
| 20180924B | $90.2 \pm 2.0$ | $-13.3 \pm 1.4$ | $22 \pm 2$ | $7 \pm 9$ | Day et al. [61] |
| 20181112A | 90 | 10 | $10.9 \pm 0.9$ | – | Prochaska et al. [88] |
| 20190102C | $82.3 \pm 0.7$ | $4.8 \pm 0.5$ | $-105 \pm 1$ | $34 \pm 22$ | Day et al. [61] |
| 20190303A | ≥20 | – | $-499.8 \pm 0.7$ | $14 \pm 5$ | Fonseca et al. [56] |
| 20190606A | 100 | – | $-20 \pm 1$ | $13 \pm 5$ | Fonseca et al. [56] |
| 20190608B | $91 \pm 3$ | $-9 \pm 2$ | $353 \pm 2$ | $-25 \pm 8$ | Day et al. [61] |
| 20190611B | $93 \pm 3$ | $15 \pm 2$ | $20 \pm 4$ | $30 \pm 19$ | Day et al. [61] |
| 20190711A | $101 \pm 2$ | $-1 \pm 2$ | $9 \pm 2$ | $27 \pm 20$ | Day et al. [61] |
| 20191108A | 70 | ≤10 | $474 \pm 3$ | −50 | Connor et al. [98] |
| 20201124A | 91 | 6 | $-601 \pm 11$ | $-57 \pm 33$ | Hilmarsson et al. [180] |

In addition to the RMs, the polarization position angle (PA) across the burst phase offer additional diagnostic information for informing FRB emission models. According to the rotating vector model for pulsars, we expect the PA to trace an S-shaped curve as the beam of radiation crosses the observer's line of sight. Some apparently one-off FRBs exhibit variable polarisation position angles e.g., FRB 20110523A [48]. On the contrary, most repeating FRBs which have polarisation information in the literature, have constant PAs during each burst (e.g., FRBs 20121102A [165], 20180916B [57], 20190711A [61], 20190604A [56], 20190303A [56]). In the case of repeating FRBs, it could just reflect timescale and altitude of the emission process rather than the rate of a rotating beam sweeping across the line of sight, like in the case of most radio loud magnetars which are observed to have flat PAs [163]. Variable PAs have also been observed in a radio loud magnetar as shown in Kramer et al. [181]. An outlier in the polarised sample of repeaters is FRB 20180301A, whose pulses show a rich diversity of PA swings across the pulse profiles [103]. This diversity is consistent with a magnetospheric origin of the radio emission, and disfavours the radiation models invoking relativistic shocks [103] similar to what has been suggested for FRB 20180916B [62]. Noteworthily, giant pulses from the Crab pulsar exhibit constant PAs in their high frequency interpulse mode, but show variable PA swings in the normal main pulse mode [163,182].

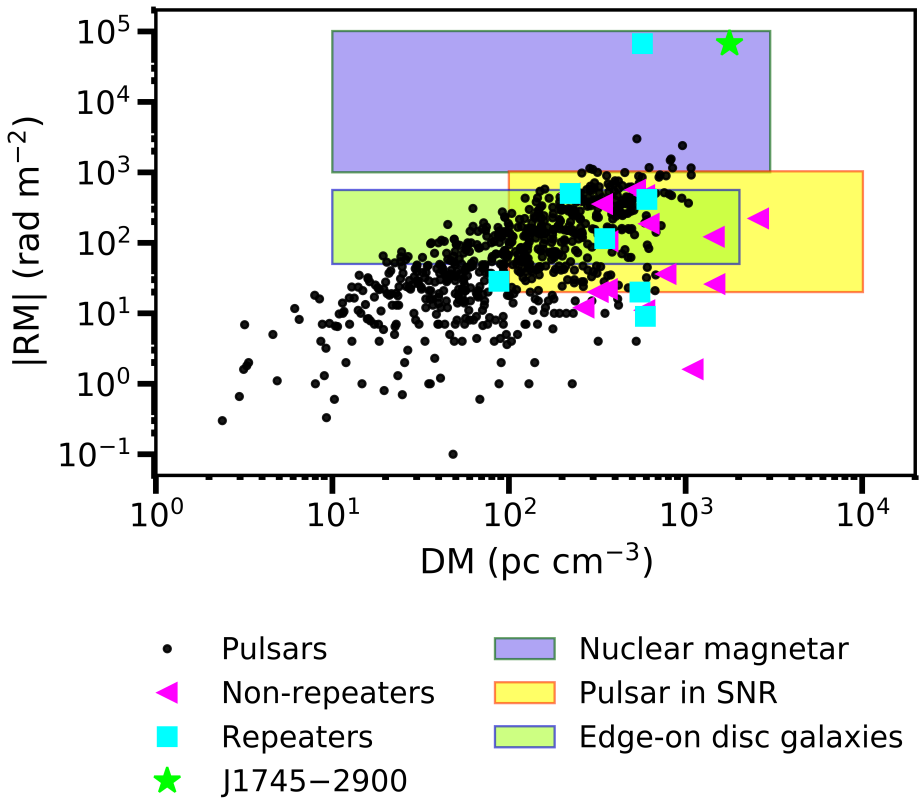


**Figure 6.** Comparison of the DMs and RMs of pulsars and FRBs. The FRB DMs are upper limits as they are the total observed values. The shaded regions indicate various progenitor models in RM–DM space. The similarity of the RM of FRB 20121102A to that of the Galactic centre magnetar J1745−2900 suggests an association with an AGN for the FRB.

### *5.10. Pulse Widths*

An interesting property of FRBs are their pulse widths, which give us an understanding of the progenitor physics and the medium the signal has travelled through. The observed pulse width ($W$) of an FRB is the sum of various contributing factors along the line-of-sight and at the telescope given by,

$$W^2 = \tau_{\rm IGM}^2 + \tau_{\rm ISM}^2 + \tau_{\rm int}^2 + \tau_{\rm DM}^2 + \tau_{\delta \rm DM}^2 + \tau_{\rm samp}^2 + \tau_{\delta\nu}^2, \quad (14)$$

where the first two components are the scattering times due to the IGM and ISM, $\tau_{\rm int}$ is the (unknown) intrinsic width of the pulse, $\tau_{\rm DM}$ is due to the DM smearing, $\tau_{\delta \rm DM}$ is the second order correction to the DM smearing, $\tau_{\rm samp}$ is due to the adopted sampling time and $\tau_{\delta\nu}$ is the filter response of an individual frequency channel [27]. The observed widths of FRBs discovered to data range from ≈10 µs to 40 ms. The intrinsic temporal pulse width may observationally distinguish repeating and as-yet non-repeating FRBs as initially noted in Scholz et al. [183]. They found that the intrinsic widths of a sample of FRB 20121102A bursts were broader than a sample of apparently non-repeating FRBs detected with the Parkes telescope. Similarly, Fonseca et al. [56] compared the widths of a sample of repeater and non-repeater pulses of S/N $\geq$ 10 detected by the CHIME telescope in the 400–800 MHz-frequency range. A self-consistent sample was chosen as the variation of intrinsic width with observing frequency is not yet well understood. The two samples do not appear to be drawn from the same distribution, suggesting different origins. More recently, based on the CHIME catalog of ∼550 sources, Pleunis, Ziggy and Good, Deborah C. and Kaspi, Victoria M. and Mckinven, Ryan and Ransom, Scott M. and Scholz, Paul and Bandura, Kevin and Bhardwaj, Mohit and Boyle, P. J. and Brar, Charanjot and Cassanelli, Tomas and Chawla, Pragya and Fengqiu and Dong and Fonseca, Emmanuel

and Gaensler, B. M. and Josephy, Alexander and Kaczmarek, Jane F. and Leung, Calvin and Lin, Hsiu-Hsien and Masui, Kiyoshi W. and Mena-Parra, Juan and Michilli, Daniele and Ng, Cherry and Patel, Chitrang and Rafiei-Ravandi, Masoud and Rahman, Mubdi and Sanghavi, Pranav and Shin, Kaitlyn and Smith, Kendrick M. and Stairs, Ingrid H. and Tendulkar, Shriharsh P., [184] report that in addition to being broader in width, repeaters on average emit in small spectral bands compared to non-repeaters. This is visualised in Figure 7, which shows the bandwidths and durations of the FRBs with S/N $>$ 12. Similarly, Qiu et al. [160] studied the profiles of 33 bright FRBs detected by ASKAP. Their stacked normalised posterior distribution of intrinsic pulse widths from the ASKAP sample contain seven FRBs with measurable intrinsic pulse widths including two ASKAP repeaters. Unlike in the CHIME sample, Qiu et al. [160] do not see any evidence for bimodality in the pulse width distribution. However, it should be noted that this is a much smaller sample of repeaters compared to CHIME. While the bimodal distribution is suggestive of two origins, it could potentially be a selection effect of repeating FRBs having wider beaming angles, which would make repetitions more likely to be detected. The pulse width distribution should be interpreted with caution as repeating FRBs tend to be broader due to drifting sub-bursts. We have also seen in Section 5.8.4 that not all repeaters show sub-bursts and it is possible that these apparently non-repeaters could exhibit broader repeat pulses.

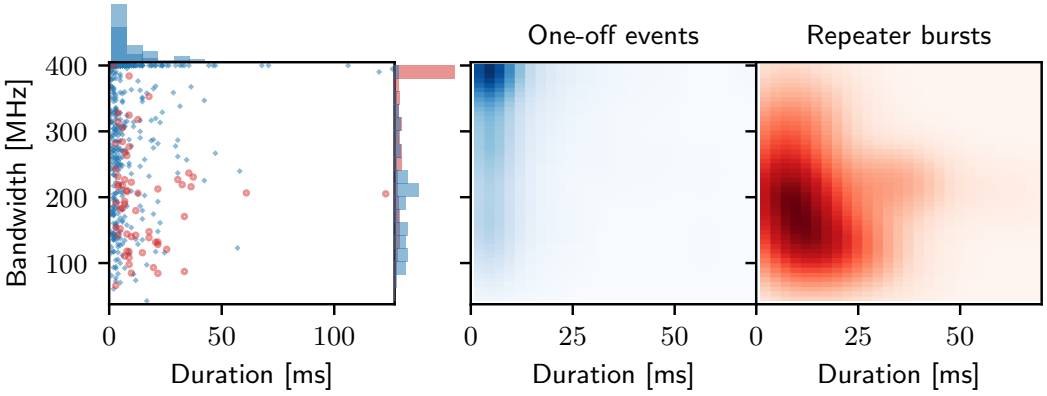


**Figure 7.** Comparison of the bandwidths and durations of the FRBs in the CHIME Catalog 1. Blue diamonds represent one-off events and red open circles denote repeater pulses. The normalised histograms on the right show that one-off events are narrower in width and occupy a larger bandwidth compared to repeater bursts, which are broader in width and occupy a comparatively smaller bandwidth. One-off events may potentially be as-of-yet undiscovered repeaters (e.g., due to limited exposure or source activity). Figure credit: Ziggy Pleunis.

### *5.11. Host Galaxies and Progenitors*

The scientific payoff from an astrophysical source is only truly realised upon localisation. Most FRBs discovered during the early stages of the field were detected with single pixel radio telescopes with relatively poor angular resolution. As a result, most of the initial discoveries were poorly localised. With the advent of interferometers and discoveries of repeating FRBs, localisations and associations with host galaxies have become more common. FRB 20121102A was the first one to be localised due to its repeating nature. It is seen to lie in a star forming region in the outskirts of the dwarf galaxy at a redshift of $z = 0.19273(8)$, and is offset from the centre of light of the galaxy. The sub-milliarcsecond localisation of the first repeating FRB 20121102A with high rotation measure (see Section 5.9) showed that it is physically associated with a compact ($<$0.7 pc), persistent radio source exhibiting $\sim$10% variability on day timescales, which appears to provide important clues to the origin of the radio bursts [50,52]. The persistent radio source associated with the FRB location is visible all the way from 1 to 26 GHz and might be key to understanding the energetics and the formation of the FRB source. For instance, a roughly decade-old, highly magnetised neutron star could be injecting energy into the

surrounding medium, producing a luminous magnetar wind nebula [185]. Some have suggested that the radio bursts are produced not in the magnetar's magnetosphere, but at the interface of the magnetar wind and surrounding environment [185,186]. In this case, FRBs may always be associated with compact, persistent radio sources. Following this discovery several searches ensued for FRBs in dwarf galaxies with similar conditions to that of FRB 20121102A, but no new FRBs were discovered. Recently, a second repeating FRB source, FRB 20180916B was precisely localised to the apex of an apparently 'V'-shaped star-forming region in a nearby massive galaxy at $z = 0.0337$ [187], using the European VLBI Network of telescopes. Interestingly, FRBs 20121102A and FRB 20180916B are in close proximity to star-forming regions of sizes 1.4–1.9 kpc and 380 pc respectively within their host galaxies, with offsets of $\sim$250 pc from the peak of star-formation of these regions [188]. However, the lack of both a comparably luminous persistent radio counterpart and a high Faraday rotation measure distinguishes FRB 20180916B from FRB 20121102A. In contrast, the repeating FRB 20200120E is observed to be associated with a globular cluster in the M81 galactic system [189]. Since globular clusters typically host an older stellar population, this association challenges FRB models involving magnetars formed through the standard core-collapse supernova channel. However, a magnetar formed either through accretion induced collapse or a merger of compact stars in a binary system are still viable, as are giant pulses from millisecond pulsars [189]. Additionally, heightened activity from the repeating FRB 20201124A enabled it to be localised to a host galaxy at a redshift of $z = 0.098 \pm 0.002$ [190]. Similar to FRB 20121102A, persistent radio emission from FRB 20201124A was detected by the uGMRT [191] and the JVLA [192] on angular scales of a few arcseconds but resolved out at scales of $\sim$0.1 arcseconds with the European VLBI Network [193]. This demonstrates that repeating FRBs have a wide range of luminosities, and originate from diverse host galaxies and local environments.

In contrast to the repeaters, the Australian SKA Pathfinder (ASKAP) [89,194], DSA-10 [99] and VLA [195] telescopes have localised several one-off FRBs to host galaxies through imaging of buffered raw-voltage data. Of all the known FRBs, only 19 have been localised to host galaxies[4] with spectroscopic redshift measurements [196] in the range of $z\sim$0.0001–0.66. The increasing arcsecond localisations of one-off events in addition to repeaters suggests that we are entering an era where we can begin to look for evidence of multiple classes by studying FRB host galaxies and potential multi-wavelength counterparts. The host galaxies of FRB 20180916B [187] and other non-repeating bursts [194] with more massive and older stellar populations, are strikingly different in their properties compared to the host of FRB 20121102A. The location of the apparently non-repeating FRB 20190608B within its spiral host galaxy at a redshift of $z = 0.11778$ [197], is remarkably similar to that of the repeating FRB 20180916B. However, further investigation of their similarities would require milliarcsecond localisation obtained from potential repeat bursts.

Heintz et al. [194], Bhandari et al. [198] and Li and Zhang [199] studied the global properties of a sample of host galaxies comprising repeating and one-off FRBs. The host galaxies of FRBs are seen to range from from starburst to nearly quiescent. They find that the physical offset between the FRB positions and the host galaxy centers range from 0.6 to 11 kpc, with a median value of 3.3 kpc. Overall, FRBs are not seen to occur in the nuclei of their hosts. High spatial resolution images show most FRBs to be located in the arms of these galaxies [200]. These physical offsets shown in Figure 8 are consistent with those observed for short Gamma-ray bursts, core-collapse supernovae, and Type Ia supernovae suggesting that FRB progenitors host population shares the similar characteristics to those of these transients. Magnetars formed via regular core-collapse supernovae, binary neutron star mergers and accretion-induced collapses of white dwarfs are plausible progenitors to the FRBs in this sample [194,201]. The current sample of FRB host galaxies are moderately star forming with star formation rates in the range 0.03–8$M_\odot$ $yr^{-1}$. These are statistically inconsistent with the star formation rates of ULXs and Type Ia supernovae host galaxies, which are often more star forming (see Figure 8).

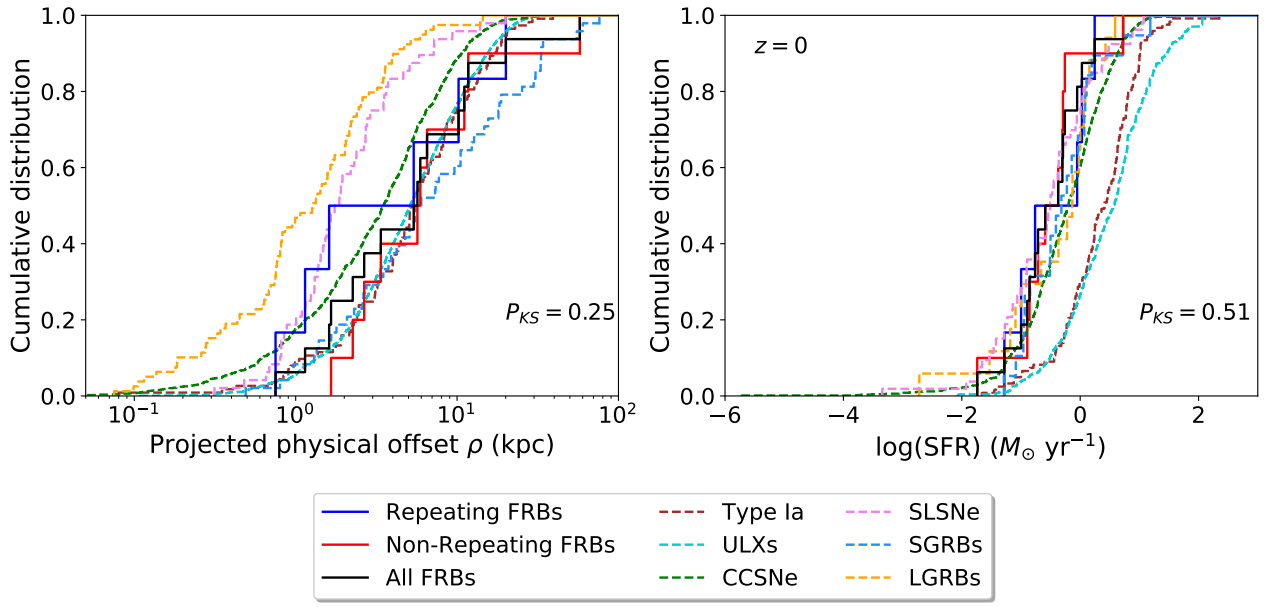


**Figure 8.** Cumulative distributions of the projected physical offsets and star formation rates for the FRBs and various classes of transients. The p-values for a Kolmogorov-Smirnoff test between the repeating and non-repeating population is listed in each plot. The star-formation rates of host galaxies of FRBs and other transients are redshift corrected to be statistically representative of $z = 0$ galaxies. Figure credit: Shivani Bhandari.

A Baldwin, Phillips & Telervich BPT [202] diagram (the ratios of measured line fluxes for [O III]/H$\beta$ against [N II]/H$\alpha$ and [S II]/H$\alpha$) compares the hosts of FRBs with star-forming galaxies, low-ionization nuclear emission line region (LINER) galaxies, and active galactic nuclei (AGN). Figure 9 shows the BPT diagram for a sample of well-localised FRBs reported in Heintz et al. [194] and Bhandari et al. [198]. The majority of FRB hosts are emission-line galaxies that appear to favour AGN and LINER populations. The FRBs in Figure 9 do not track the stellar mass and overall are not hosted in old, red and dead galaxies which possess an older stellar population. The present data supports a mix of prompt (core-collapse supernovae) and delayed channels for producing FRB progenitors [198]. Currently, even with the addition of the Galactic magnetar SGR 1935 + 2154 to the repeating FRB class, there is no distinction between the hosts of repeaters and one-off FRBs [199]. Little is known about the radio properties of these galaxies as only a few FRB host galaxies have been detected in the radio. While both repeating and apparently one-off FRBs have, and are continuing to be localised, the connection between them (if any) remains unclear at the moment and therefore understanding their host galaxies and immediate environments is crucial.

### *5.12. Afterglows and Persistent Emission*

Synchrotron radio emission is a distinctive feature of jets of ejecta or expanding shells, and is well observed in GRBs and supernovae. Typically, radio emission is only observable once the ejecta become optically thin. FRB 20121102A is the only FRB where persistent emission has been detected, despite follow-up observations of other localised FRBs reaching lower luminosity limits. No persistent radio emission was found to be associated with FRB 20180916A above a 3-sigma r.m.s. noise level of 30 µJy beam$^{-1}$ with the EVN at 1.7 GHz and a 3-sigma r.m.s. noise level of 18 µJy beam$^{-1}$ with the VLA at 1.6 GHz [187]. Any persistent radio emission in the vicinity of FRB20180916A would be 400 times fainter than the one associated with FRB 20121102A [52]. Similarly, no persistent radio emission was detected at the position of the Galactic magnetar in MeerKAT radio images at 1.4 GHz above 103 µy beam$^{-1}$ [203]. Four of the FRBs discovered and localised by the ASKAP telescope were observed within 10 days of the bursts' discoveries with the Australian Telescope Compact Array (ATCA) at centre frequencies of 5.5 and 7.5 GHz [204]. After combining

the data from the two bands, Bhandari et al. [204] found no continuum emission anywhere within the host galaxies of FRB 20180924B, FRB 20181112A, or FRB 20190102C ($S_{6.5\mathrm{GHz}} <\sim 20$ μJy) and no continuum emission at the location of FRB 20190608B within its host ($S_{6.5\mathrm{GHz}} <\sim 10$ μJy). uGMRT observations of the repeating FRB 20201124A detected an unresolved persistent radio source with a 650 MHz flux density of $0.7 \pm 0.1$ mJy. Subsequent JVLA imaging in the S and X bands detected an unresolved persistent radio source with a flux density of $0.34 \pm 0.03$ mJy at 3 GHz and $0.15 \pm 0.01$ mJy at 9 GHz coincident with the uGMRT detection. EVN observations of the field ruled out any emission on angular scales larger than $\gtrsim$140 mas, thereby suggesting that the persistent emission detected by the uGMRT and the JVLA must be extended in nature [193]. A combination of the global properties of the host galaxies and the existence/non-existence of persistent emission will help constrain a possible correlation between source age and existence of persistent emission, and help address the question of multiple populations.

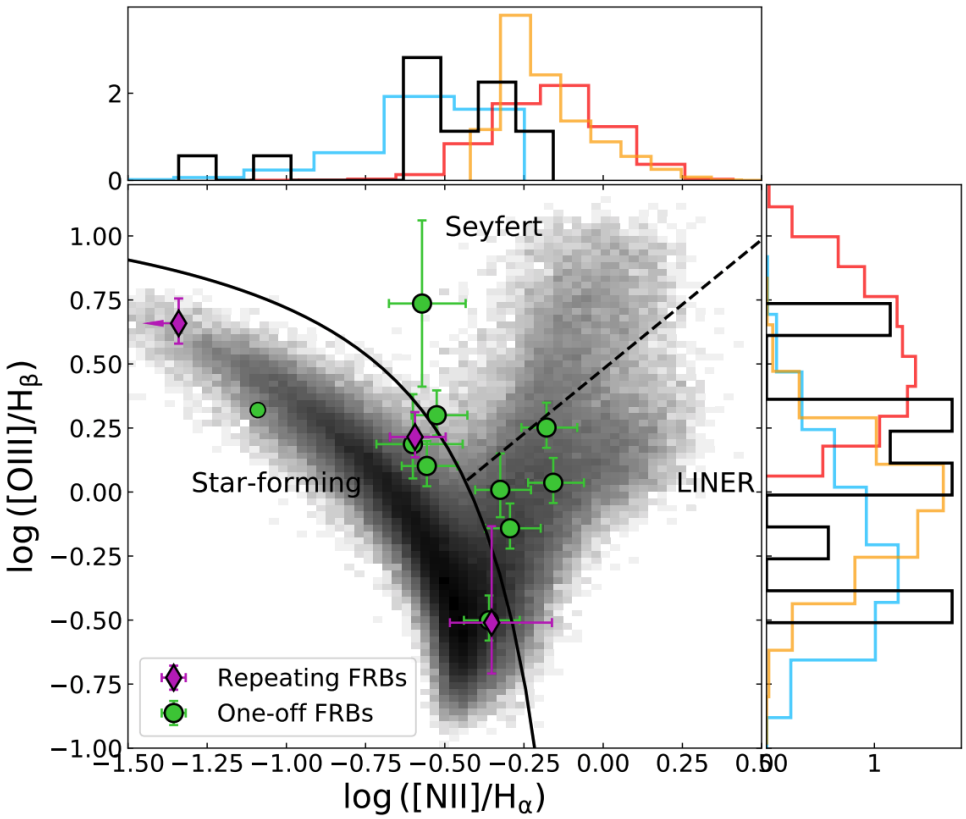


**Figure 9.** Emission line properties for the host galaxies of a sample of well-localised FRBs compared to star-forming galaxies, LINER galaxies, and AGN. Sample A corresponds to highly probable host-galaxy associations based on the FRB localization and galaxy photometry. Most FRB hosts are observed to lie away from star-forming main sequence and are concentrated more towards LINER galaxies. The host galaxy of FRB 121102 is an obvious outlier lying close to the tail-end of the stat-forming sequence. Figure credit: Shivani Bhandari.

## 6. Biases in Observations and Detections

While modelling and interpreting the properties of FRBs, it is important to recognise several, quite different selection effects and observational biases. These incompleteness factors are important in determining accurate underlying population characteristics, e.g., [205,206] and the use of FRBs in cosmological studies. Below, we summarise a few of the main biases in our current studies of FRB populations.

- The expected detection rate at a telescope for any observation depends on the DM range searched combined with the frequency resolution of the observations. Coarser frequency resolution causes observations to be less sensitive to high-DM FRB events due to DM smearing [141,206].
- Any given telescope is incomplete to FRB detections below a certain threshold fluence. Pulses with the same fluence but different widths (due to propagation effects) are not equally detectable as search algorithms become increasingly incomplete to wide bursts. Even if FRBs are not broader than the widths searched at telescopes, they may still be incomplete in fluence. It is crucial to account for fluence completeness in source count distribution estimates [205].
- The effects of attenuation by the unknown position in the telescope beam response is reflected in the amplitude of the source count slope. Any estimation of the source count slope therefore requires that either all events are corrected for the effect of beam attenuation, or that corrections are applied to no events. It should be noted that fully-sampled focal-plane arrays do have this problem [41].

## 7. Summary and Future Prospects

The field of FRBs started on shaky ground followed by a roller coaster ride, but has since grown richer, and holds exciting prospects. The last few years have revolutionized FRB astronomy and we as a community are on the brink of answering some of the most fundamental open questions regarding their nature and applications in other areas of astrophysics. Presently, new FRBs (both repeating and non-repeating) continue to be steadily discovered with existing instrumentation. Over 50 progenitor model theories have been proposed for FRBs, ranging from flaring magnetars and the destruction of highly magnetised white dwarfs, to more exotic ones involving interactions between axion stars and black holes. The only stringent limitation for a model progenitor is that the FRB cannot be embedded in a medium too dense that gigahertz-frequency emissions would be suppressed. We know that FRBs are detectable as low as 110 MHz and as high as 8 GHz, though not yet across a wide and continuous range of frequencies. With the detection of FRB like pulses from a Galactic magnetar, we now know that at least a sub-population of FRBs can be produced by extragalactic/cosmological magnetars. The diversity in the morphology of the existing sample of host galaxies and the locations of FRBs within them, makes it important to study a larger sample to discern their origins.

Ongoing and planned real-time identifications of FRBs will permit quasi-real-time triggering of multi-wavelength instruments to search for afterglows through automated mechanisms such as VOEvents. Detections of gravitational waves associated with an FRB would actually prove its cataclysmic nature and provide a direct link with neutron star mergers, gamma-ray bursts and kilonovae. The detection of gravitational waves in association with FRBs could be relevant to repeaters as well, e.g., magnetospheric interactions decades to centuries before the merger can make repeating FRBs while emitting gravitational waves [207]; and a post-merger magnetar sometime after the coalescence could make repeating FRBs [208,209]. In the latter case, a historical gravitational wave source can be associated with a repeater. Neutrino detections coincident with FRBs on the other hand, would give us insight into hadronic accelerations and atomic decay processes associated with the source [210]. The better we can characterize the radio bursts and their associated multi-wavelength emission, the better our chances are of identifying the underlying emission mechanism. The full potential of FRBs will only be realized in the era of routine FRB detections and corresponding host galaxy identifications. The MeerKAT telescope in South Africa through the MeerTRAP[5] and TRAPUM[6] projects have started scanning the skies for FRBs along with the robotic MeerLICHT optical telescope to identify possible contemporaneous optical flashes that FRBs might produce. The STARE2, UTMOST, ASKAP and CHIME telescopes are making significant advances in studying the low DM (100–1000 pc $cm^{-3}$) population in the relatively local Universe. The ASKAP, DSA-10 and VLA telescopes are making huge strides towards real time detections and localisations.

Upcoming wide-field telescopes such as the Canadian Hydrogen Observatory and Radio transient Detector (CHORD), Hydrogen Intensity and Real-time Analysis experiment (HIRAX) and the SKA are expected to deliver hundreds if not thousands of localised FRBs across a range of redshifts. In or near 2023, we will also have initial FRB survey results from the next generation telescopes like FAST and MeerKAT which will push our search horizons beyond redshifts of 2. While high-$z$ FRBs hold great potential for cosmological studies, low-$z$ FRBs are better observationally. We can expect multiple new detections, host galaxy identifications and physical insights in the next few years. The future of FRB science is certainly very bright and we can expect an abundance of exciting science in the coming years.

**Author Contributions:** Conceptualisation and methodology, M.C., E.K.; writing—original draft preparation, M.C.; writing—review and editing, M.C., E.K. All authors have read and agreed to the published version of the manuscript.

**Funding:** M.C. acknowledges funding from the European Research Council (ERC) under the European Union's Horizon 2020 research and innovation programme (grant agreement No. 694745).

**Institutional Review Board Statement:** Not applicable.

**Informed Consent Statement:** Not applicable.

**Data Availability Statement:** No new data were created or analyzed in this study. Data sharing is not applicable to this article.

**Acknowledgments:** We thank the referees for their helpful comments and suggestions which have improved the quality of the manuscript. M.C. would like to thank Chris Flynn, Benjamin Stappers and Kaustubh Rajwade for useful discussion and feedback on the manuscript. M.C. is grateful to Wael Farah for providing the data from FRB 20181017C in Figure 5, and Ziggy Pleunis and Shivani Bhandari for the use of figures.

**Conflicts of Interest:** The authors declare no conflict of interest. The funders had no role in the design of the study; in the collection, analyses, or interpretation of data; in the writing of the manuscript, or in the decision to publish the results.

## Abbreviations

The following abbreviations are used in this manuscript:

| | |
|---|---|
| AGN | Active Galactic Nuclei |
| ASKAP | Australian Square Kilometre Array Pathfinder |
| ATCA | Australian Telescope Compact Array |
| CGM | Circumgalactic medium |
| BPT | Baldwin, Phillips & Telervich |
| CHIME | Canadian Hydrogen Intensity Mapping Experiment |
| DM | Dispersion measure |
| DSA | Deep Synoptic Array |
| EVN | European Very Long Baseline Interferometry Network |
| FAST | Five-hundred-meter Aperture Spherical Telescope |
| FRB | Fast radio burst |
| GBT | Green Bank telescope |
| GMRT | Giant Metrewave Radio Telescope |
| GRB | Gamma-Ray Burst |
| IGM | Intergalactic medium |
| ISM | Interstellar medium |
| LINER | Low-Ionization Nuclear Emission Region |
| LOFAR | Low-Frequency Array |

| | |
|---|---|
| LGRBs | Long Gamma-Ray bursts |
| MWA | Murchison Widefield Array |
| RM | Rotation measure |
| SGBRs | Short Gamma-Ray bursts |
| SRT | Sardinia Radio telescope |
| STARE2 | Survey for Transient Astronomical Radio Emission 2 |
| SKA | Square Kilometer Array |
| VLA | Very Large Array |
| WSRT | Westerbork Synthesis Radio Telescope |

## Notes

1 As of March 2020 this has been replaced by the Transient Naming Server convention as FRB YYYYMMDDabc.
2 It is common to refer to the fluence density of FRBs incorrectly as simply fluence, we do likewise.
3 https://www.wis-tns.org/, accessed on 25 June 2021.
4 https://frbhosts.org/, accessed on 22 September 2021.
5 https://www.meertrap.org/, accessed on 26 January 2021.
6 http://www.trapum.org/, accessed on 26 January 2021.

## References


1. Hankins, T.H.; Eilek, J.A. Radio Emission Signatures in the Crab Pulsar. *Astrophys. J.* **2007**, *670*, 693–701. [CrossRef]
2. Galama, T.J.; Vreeswijk, P.M.; van Paradijs, J.; Kouveliotou, C.; Augusteijn, T.; Böhnhardt, H.; Brewer, J.P.; Doublier, V.; Gonzalez, J.F.; Leibundgut, B.; et al. An unusual supernova in the error box of the $\gamma$-ray burst of 25 April 1998. *Nature* **1998**, *395*, 670–672. [CrossRef]
3. Lyubarsky, Y. Emission Mechanisms of Fast Radio Bursts. *Universe* **2021**, *7*, 56. [CrossRef]
4. Nicastro, L.; Guidorzi, C.; Palazzi, E.; Zampieri, L.; Turatto, M.; Gardini, A. Multiwavelength Observations of Fast Radio Bursts. *Universe* **2021**, *7*, 76. [CrossRef]
5. Bhandari, S.; Flynn, C. Probing the Universe with Fast Radio Bursts. *Universe* **2021**, *7*, 85. [CrossRef]
6. Whelan, J.; Iben, I., Jr. Binaries and Supernovae of Type I. *Astrophys. J.* **1973**, *186*, 1007–1014. [CrossRef]
7. Perlmutter, S.; Aldering, G.; Goldhaber, G.; Knop, R.A.; Nugent, P.; Castro, P.G.; Deustua, S.; Fabbro, S.; Goobar, A.; Groom, D.E.; et al. Measurements of $\Omega$ and $\Lambda$ from 42 High-Redshift Supernovae. *Astrophys. J.* **1999**, *517*, 565–586. [CrossRef]
8. Riess, A.G.; Filippenko, A.V.; Challis, P.; Clocchiatti, A.; Diercks, A.; Garnavich, P.M.; Gilliland, R.L.; Hogan, C.J.; Jha, S.; Kirshner, R.P.; et al. Observational Evidence from Supernovae for an Accelerating Universe and a Cosmological Constant. *Astron. J.* **1998**, *116*, 1009–1038. [CrossRef]
9. Hewish, A.; Bell, S.J.; Pilkington, J.D.H.; Scott, P.F.; Collins, R.A. Observation of a Rapidly Pulsating Radio Source. *Nature* **1968**, *217*, 709–713. [CrossRef]
10. Hulse, R.A.; Taylor, J.H. Discovery of a pulsar in a binary system. *Astrophys. J.* **1975**, *195*, L51–L53. [CrossRef]
11. Klebesadel, R.W.; Strong, I.B.; Olson, R.A. Observations of Gamma-Ray Bursts of Cosmic Origin. *Astrophys. J.* **1973**, *182*, L85. [CrossRef]
12. Cucchiara, A.; Levan, A.J.; Fox, D.B.; Tanvir, N.R.; Ukwatta, T.N.; Berger, E.; Krühler, T.; Küpcü Yoldaş, A.; Wu, X.F.; Toma, K.; et al. A Photometric Redshift of z ~9.4 for GRB 090429B. *Astrophys. J.* **2011**, *736*, 7. [CrossRef]
13. Smartt, S.J.; Chen, T.W.; Jerkstrand, A.; Coughlin, M.; Kankare, E.; Sim, S.A.; Fraser, M.; Inserra, C.; Maguire, K.; Chambers, K.C.; et al. A kilonova as the electromagnetic counterpart to a gravitational-wave source. *Nature* **2017**, *551*, 75–79. [CrossRef] [PubMed]
14. Lorimer, D.R.; Bailes, M.; McLaughlin, M.A.; Narkevic, D.J.; Crawford, F. A Bright Millisecond Radio Burst of Extragalactic Origin. *Science* **2007**, *318*, 777–780. [CrossRef] [PubMed]
15. Thornton, D.; Stappers, B.; Bailes, M.; Barsdell, B.; Bates, S.; Bhat. A Population of Fast Radio Bursts at Cosmological Distances. *Science* **2013**, *341*, 53–56. [CrossRef] [PubMed]
16. Linscott, I.R.; Erkes, J.W. Discovery of millisecond radio bursts from M 87. *Astrophys. J. Lett.* **1980**, *236*, L109–L113. [CrossRef]
17. Hankins, T.H.; Campbell, D.B.; Davis, M.M.; Ferguson, D.C.; Sieber, W.; Neidhoefer, J.; Wright, G.A.E.; Ekers, R.; Osullivan, J. Searches for the radio millipusles from M 87 Virgo A. *Astrophys. J. Lett.* **1981**, *244*, L61–L64. [CrossRef]
18. McLaughlin, M.A.; Lyne, A.G.; Lorimer, D.R.; Kramer, M.; Faulkner, A.J.; Manchester, R.N.; Cordes, J.M.; Camilo, F.; Possenti, A.; Stairs, I.H.; et al. Transient radio bursts from rotating neutron stars. *Nature* **2006**, *439*, 817–820. [CrossRef]
19. Staveley-Smith, L.; Wilson, W.E.; Bird, T.S.; Disney, M.J.; Ekers, R.D.; Freeman, K.C.; Haynes, R.F.; Sinclair, M.W.; Vaile, R.A.; Webster, R.L.; et al. The Parkes 21 CM multibeam receiver. *Publ. Astron. Soc. Aust.* **1996**, *13*, 243–248. [CrossRef]
20. Kulkarni, S.R. Dispersion measure: Confusion, Constants & Clarity. *arXiv* **2020**, arXiv:2007.02886.
21. Hogg, D.W. Distance measures in cosmology. *arXiv* **1999**, arXiv:astro-ph/9905116.
22. Deng, W.; Zhang, B. Cosmological Implications of Fast Radio Burst/Gamma-Ray Burst Associations. *Astrophys. J. Lett.* **2014**, *783*, L35. [CrossRef]

23. Ade, P. A.; Aghanim, N.; Arnaud, M.; Ashdown, M.; Aumont, J.; Baccigalupi, C.; Banday, A.J.; Barreiro, R.B.; Bartlett, J.G.; Matarrese, S.; et al. Planck 2015 results. XIII. Cosmological parameters. *Astron. Astrophys.* **2016**, *594*, A13. [CrossRef]
24. Fukugita, M.; Hogan, C.J.; Peebles, P.J.E. The Cosmic Baryon Budget. *Astrophys. J.* **1998**, *503*, 518–530. [CrossRef]
25. Shull, J.M.; Smith, B.D.; Danforth, C.W. The Baryon Census in a Multiphase Intergalactic Medium: 30% of the Baryons May Still be Missing. *Astrophys. J.* **2012**, *759*, 23. [CrossRef]
26. Deller, A.T.; Brisken, W.F.; Chatterjee, S.; Cordes, J.M.; Goss, W.M.; Janssen, G.H.; Kovalev, Y.Y.; Lazio, T.J.W.; Petrov, L.; Stappers, B.W. PSR$\pi$: A large VLBA pulsar astrometry program. In Proceedings of the 20th Meeting of the European VLBI Group for Geodesy and Astronomy, Bonn, Germany, 29–30 March 2011; pp. 178–182.
27. Cordes, J.M.; McLaughlin, M.A. Searches for Fast Radio Transients. *Astrophys. J.* **2003**, *596*, 1142–1154. [CrossRef]
28. Yao, J.M.; Manchester, R.N.; Wang, N. A New Electron-density Model for Estimation of Pulsar and FRB Distances. *Astrophys. J.* **2017**, *835*, 29. [CrossRef]
29. Dolag, K.; Gaensler, B.M.; Beck, A.M.; Beck, M.C. Constraints on the distribution and energetics of fast radio bursts using cosmological hydrodynamic simulations. *Mon. Not. R. Astron. Soc.* **2015**, *451*, 4277–4289. [CrossRef]
30. Yamasaki, S.; Totani, T. The Galactic Halo Contribution to the Dispersion Measure of Extragalactic Fast Radio Bursts. *Astrophys. J.* **2020**, *888*, 105. [CrossRef]
31. Keating, L.C.; Pen, U.L. Exploring the dispersion measure of the Milky Way halo. *Mon. Not. R. Astron. Soc.* **2020**, *496*, L106–L110. [CrossRef]
32. Ioka, K. The Cosmic Dispersion Measure from Gamma-Ray Burst Afterglows: Probing the Reionization History and the Burst Environment. *Astrophys. J. Lett.* **2003**, *598*, L79–L82. [CrossRef]
33. Zheng, Z.; Ofek, E.O.; Kulkarni, S.R.; Neill, J.D.; Juric, M. Probing the Intergalactic Medium with Fast Radio Bursts. *Astrophys. J.* **2014**, *797*, 71. [CrossRef]
34. Keane, E.F. The future of fast radio burst science. *Nat. Astron.* **2018**, *2*, 865–872. [CrossRef]
35. Zhang, B. Fast Radio Burst Energetics and Detectability from High Redshifts. *Astrophys. J. Lett.* **2018**, *867*, L21. [CrossRef]
36. McQuinn, M. Locating the "Missing" Baryons with Extragalactic Dispersion Measure Estimates. *Astrophys. J. Lett.* **2014**, *780*, L33. [CrossRef]
37. James, C.W.; Prochaska, J.X.; Macquart, J.P.; North-Hickey, F.; Bannister, K.W.; Dunning, A. The z–DM distribution of fast radio bursts. *arXiv* **2021**, arXiv:2101.08005.
38. Keane, E.F.; Stappers, B.W.; Kramer, M.; Lyne, A.G. On the origin of a highly dispersed coherent radio burst. *Mon. Not. R. Astron. Soc.* **2012**, *425*, L71–L75. [CrossRef]
39. Bannister, K.W.; Madsen, G.J. A Galactic origin for the fast radio burst FRB010621. *Mon. Not. R. Astron. Soc.* **2014**, *440*, 353–358. [CrossRef]
40. Keith, M.J.; Jameson, A.; van Straten, W.; Bailes, M.; Johnston, S.; Kramer, M.; Possenti, A.; Bates, S.D.; Bhat, N.D.R.; Burgay, M.; et al. The High Time Resolution Universe Pulsar Survey—I. System configuration and initial discoveries. *Mon. Not. R. Astron. Soc.* **2010**, *409*, 619–627. [CrossRef]
41. Macquart, J.P.; Ekers, R.D. Fast radio burst event rate counts—I. Interpreting the observations. *Mon. Not. R. Astron. Soc.* **2018**, *474*, 1900–1908. [CrossRef]
42. Lyutikov, M. Fast Radio Bursts' Emission Mechanism: Implication from Localization. *Astrophys. J. Lett.* **2017**, *838*, L13. [CrossRef]
43. Luo, R.; Men, Y.; Lee, K.; Wang, W.; Lorimer, D.R.; Zhang, B. On the FRB luminosity function—II. Event rate density. *Mon. Not. R. Astron. Soc.* **2020**, *494*, 665–679. [CrossRef]
44. Zhang, B. The physical mechanisms of fast radio bursts. *Nature* **2020**, *587*, 45–53. [CrossRef] [PubMed]
45. Ravi, V.; Shannon, R.M.; Jameson, A. A Fast Radio Burst in the Direction of the Carina Dwarf Spheroidal Galaxy. *Astrophys. J. Lett.* **2015**, *799*, L5. [CrossRef]
46. Spitler, L.G.; Cordes, J.M.; Hessels, J.W.T.; Lorimer, D.R.; McLaughlin, M.A.; Chatterjee, S.; Crawford, F.; Deneva, J.S.; Kaspi, V.M.; Wharton, R.S.; et al. Fast Radio Burst Discovered in the Arecibo Pulsar ALFA Survey. *Astrophys. J.* **2014**, *790*, 101. [CrossRef]
47. Petroff, E.; Bailes, M.; Barr, E.D.; Barsdell, B.R.; Bhat, N.D.R.; Bian, F.; Burke-Spolaor, S.; Caleb, M.; Champion, D.; Chandra, P.; et al. A real-time fast radio burst: Polarization detection and multiwavelength follow-up. *Mon. Not. R. Astron. Soc.* **2015**, *447*, 246–255. [CrossRef]
48. Masui, K.; Lin, H.H.; Sievers, J.; Anderson, C.J.; Chang, T.C.; Chen, X.; Ganguly, A.; Jarvis, M.; Kuo, C.Y.; Li, Y.C.; et al. Dense magnetized plasma associated with a fast radio burst. *Nature* **2015**, *528*, 523–525. [CrossRef] [PubMed]
49. Spitler, L.G.; Scholz, P.; Hessels, J.W.T.; Bogdanov, S.; Brazier, A.; Camilo, F.; Chatterjee, S.; Cordes, J.M.; Crawford, F.; Deneva, J.; et al. A repeating fast radio burst. *Nature* **2016**, *531*, 202–205. [CrossRef]
50. Chatterjee, S.; Law, C.J.; Wharton, R.S.; Burke-Spolaor, S.; Hessels, J.W.T.; Bower, G.C.; Cordes, J.M.; Tendulkar, S.P.; Bassa, C.G.; Demorest, P.; et al. A direct localization of a fast radio burst and its host. *Nature* **2017**, *541*, 58–61. [CrossRef] [PubMed]
51. Tendulkar, S.P.; Bassa, C.G.; Cordes, J.M.; Bower, G.C.; Law, C.J.; Chatterjee, S.; Adams, E.A.K.; Bogdanov, S.; Burke-Spolaor, S.; Butler, B.J.; et al. The Host Galaxy and Redshift of the Repeating Fast Radio Burst FRB 121102. *Astrophys. J. Lett.* **2017**, *834*, L7. [CrossRef]
52. Marcote, B.; Paragi, Z.; Hessels, J.W.T.; Keimpema, A.; van Langevelde, H.J.; Huang, Y.; Bassa, C.G.; Bogdanov, S.; Bower, G.C.; Burke-Spolaor, S.; et al. The Repeating Fast Radio Burst FRB 121102 as Seen on Milliarcsecond Angular Scales. *Astrophys. J. Lett.* **2017**, *834*, L8. [CrossRef]

53. Caleb, M.; Flynn, C.; Bailes, M.; Barr, E.D.; Bateman, T.; Bhandari, S.; Campbell-Wilson, D.; Farah, W.; Green, A.J.; Hunstead, R.W.; et al. The first interferometric detections of fast radio bursts. *Mon. Not. R. Astron. Soc.* **2017**, *468*, 3746–3756. [CrossRef]
54. Bannister, K.W.; Shannon, R.M.; Macquart, J.P.; Flynn, C.; Edwards, P.G.; O'Neill, M.; Osłowski, S.; Bailes, M.; Zackay, B.; Clarke, N.; et al. The Detection of an Extremely Bright Fast Radio Burst in a Phased Array Feed Survey. *Astrophys. J. Lett.* **2017**, *841*, L12. [CrossRef]
55. Bandura, K.; Addison, G.E.; Amiri, M.; Bond, J.R.; Campbell-Wilson, D.; Connor, L.; Cliche, F.; Davis, G.; Deng, M. Canadian Hydrogen Intensity Mapping Experiment (CHIME) pathfinder. In Proceedings of the Society of Photo-Optical Instrumentation Engineers (SPIE) Conference, Montreal, QC, Canada, 22–27 June 2014; Volume 9145, p. 22, [CrossRef]
56. Fonseca, E.; Andersen, B.C.; Bhardwaj, M.; Chawla, P.; Good, D.C.; Josephy, A.; Kaspi, V.M.; Masui, K.W.; Mckinven, R.; Michilli, D.; et al. Nine New Repeating Fast Radio Burst Sources from CHIME/FRB. *Astrophys. J. Lett.* **2020**, *891*, L6. [CrossRef]
57. CHIME/FRB Collaboration; Andersen, B.C.; Bandura, K.; Bhardwaj, M.; Boubel, P.; Boyce, M.M.; Boyle, P.J.; Brar, C.; Cassanelli, T.; Chawla, P.; et al. CHIME/FRB Discovery of Eight New Repeating Fast Radio Burst Sources. *Astrophys. J. Lett.* **2019**, *885*, L24. [CrossRef]
58. Palaniswamy, D.; Li, Y.; Zhang, B. Are There Multiple Populations of Fast Radio Bursts? *Astrophys. J. Lett.* **2018**, *854*, L12. [CrossRef]
59. Caleb, M.; Spitler, L.G.; Stappers, B.W. One or several populations of fast radio burst sources? *Nat. Astron.* **2018**, *2*, 839–841. [CrossRef]
60. James, C.W.; Osłowski, S.; Flynn, C.; Kumar, P.; Bannister, K.; Bhandari, S.; Farah, W.; Kerr, M.; Lorimer, D.R.; Macquart, J.P.; et al. Which bright fast radio bursts repeat? *Mon. Not. R. Astron. Soc.* **2020**, *495*, 2416–2427. [CrossRef]
61. Day, C.K.; Deller, A.T.; Shannon, R.M.; Qiu, H.; Bannister, K.W.; Bhandari, S.; Ekers, R.; Flynn, C.; James, C.W.; Macquart, J.P.; et al. High time resolution and polarization properties of ASKAP-localized fast radio bursts. *Mon. Not. R. Astron. Soc.* **2020**, *497*, 3335–3350. [CrossRef]
62. Nimmo, K.; Hessels, J.W.T.; Keimpema, A.; Archibald, A.M.; Cordes, J.M.; Karuppusamy, R.; Kirsten, F.; Li, D.Z.; Marcote, B.; Paragi, Z. Microsecond polarimetry of the repeating FRB 20180916B. *arXiv* **2020**, arXiv:2010.05800.
63. Farah, W.; Flynn, C.; Bailes, M.; Jameson, A.; Bateman, T.; Campbell-Wilson, D.; Day, C.K.; Deller, A.T.; Green, A.J.; Gupta, V.; et al. Five new real-time detections of fast radio bursts with UTMOST. *Mon. Not. R. Astron. Soc.* **2019**, *488*, 2989–3002. [CrossRef]
64. Bochenek, C.D.; Ravi, V.; Belov, K.V.; Hallinan, G.; Kocz, J.; Kulkarni, S.R.; McKenna, D.L. A fast radio burst associated with a Galactic magnetar. *arXiv* **2020**, arXiv:2005.10828.
65. Kumar, P.; Shannon, R.M.; Flynn, C.; Osłowski, S.; Bhandari, S.; Day, C.K.; Deller, A.T.; Farah, W.; Kaczmarek, J.F.; Kerr, M.; et al. Extremely band-limited repetition from a fast radio burst source. *Mon. Not. R. Astron. Soc.* **2020**. [CrossRef]
66. Keane, E.F. Classifying RRATs and FRBs. *Mon. Not. R. Astron. Soc.* **2016**, *459*, 1360–1362. [CrossRef]
67. Pleunis, Z.; Michilli, D.; Bassa, C.G.; Hessels, J.W.T.; Naidu, A.; Andersen, B.C.; Chawla, P.; Fonseca, E.; Gopinath, A.; Kaspi, V.M.; et al. LOFAR Detection of 110-188 MHz Emission and Frequency-Dependent Activity from FRB 20180916B. *arXiv* **2020**, arXiv:2012.08372.
68. Gajjar, V.; Siemion, A.P.V.; Price, D.C.; Law, C.J.; Michilli, D.; Hessels, J.W.T.; Chatterjee, S.; Archibald, A.M.; Bower, G.C.; Brinkman, C.; et al. Highest Frequency Detection of FRB 121102 at 4-8 GHz Using the Breakthrough Listen Digital Backend at the Green Bank Telescope. *Astrophys. J.* **2018**, *863*, 2. [CrossRef]
69. Sokolowski, M.; Bhat, N.D.R.; Macquart, J.P.; Shannon, R.M.; Bannister, K.W.; Ekers, R.D.; Scott, D.R.; Beardsley, A.P.; Crosse, B.; Emrich, D.; et al. No Low-frequency Emission from Extremely Bright Fast Radio Bursts. *Astrophys. J. Lett.* **2018**, *867*, L12. [CrossRef]
70. Houben, L.J.M.; Spitler, L.G.; ter Veen, S.; Rachen, J.P.; Falcke, H.; Kramer, M. Constraints on the low frequency spectrum of FRB 121102. *Astron. Astrophys.* **2019**, *623*, A42. [CrossRef]
71. Iwazaki, A. Fast Radio Bursts from Axion Stars. *arXiv* **2014**, arXiv:1412.7825.
72. Platts, E.; Weltman, A.; Walters, A.; Tendulkar, S.P.; Gordin, J.E.B.; Kandhai, S. A living theory catalogue for fast radio bursts. *Phys. Rep.* **2019**, *821*, 1–27. [CrossRef]
73. Scholz, P.; Chime/Frb Collaboration. A bright millisecond-timescale radio burst from the direction of the Galactic magnetar SGR 1935+2154. *Astron. Telegr.* **2020**, *13681*, 1.
74. CHIME/FRB Collaboration; Andersen, B.C.; Bandura, K.M.; Bhardwaj, M.; Bij, A.; Boyce, M.M.; Boyle, P.J.; Brar, C.; Cassanelli, T.; Chawla, P.; et al. A bright millisecond-duration radio burst from a Galactic magnetar. *Nature* **2020**, *587*, 54–58. [CrossRef]
75. Mereghetti, S.; Savchenko, V.; Ferrigno, C.; Götz, D.; Rigoselli, M.; Tiengo, A.; Bazzano, A.; Bozzo, E.; Coleiro, A.; Courvoisier, T.J.L.; et al. INTEGRAL discovery of a burst with associated radio emission from the magnetar SGR 1935+2154. *arXiv* **2020**, arXiv:2005.06335.
76. Li, C.K.; Lin, L.; Xiong, S.L.; Ge, M.Y.; Li, X.B.; Li, T.P.; Lu, F.J.; Zhang, S.N.; Tuo, Y.L.; Nang, Y.; et al. HXMT identification of a non-thermal X-ray burst from SGR J1935+2154 and with FRB 200428. *Nat. Astron.* **2021**, *5*, 378. [CrossRef]
77. Ridnaia, A.; Svinkin, D.; Frederiks, D.; Bykov, A.; Popov, S.; Aptekar, R.; Golenetskii, S.; Lysenko, A.; Tsvetkova, A.; Ulanov, M.; et al. A peculiar hard X-ray counterpart of a Galactic fast radio burst. *Nat. Astron.* **2021**, *5*, 372–377. [CrossRef]
78. Tavani, M.; Casentini, C.; Ursi, A.; Verrecchia, F.; Addis, A.; Antonelli, L.A.; Argan, A.; Barbiellini, G.; Baroncelli, L.; Bernardi, G.; et al. An X-ray burst from a magnetar enlightening the mechanism of fast radio bursts. *Nat. Astron.* **2021**, *5*, 401–407. [CrossRef]
79. Macquart, J.P. Probing the Universe's baryons with fast radio bursts. *Nat. Astron.* **2018**, *2*, 836–838. [CrossRef]

80. Ravi, V.; Battaglia, N.; Burke-Spolaor, S.; Chatterjee, S.; Cordes, J.; Hallinan, G.; Law, C.; Lazio, T.J.W.; Masui, K.; McQuinn, M.; et al. Fast Radio Burst Tomography of the Unseen Universe. *Bull. Am. Astron. Soc.* **2019**, *51*, 420.
81. Hackstein, S.; Brüggen, M.; Vazza, F.; Rodrigues, L.F.S. Redshift estimates for fast radio bursts and implications on intergalactic magnetic fields. *Mon. Not. R. Astron. Soc.* **2020**, *498*, 4811–4829. [CrossRef]
82. Wei, J.J.; Gao, H.; Wu, X.F.; Mészáros, P. Testing Einstein's Equivalence Principle with Fast Radio Bursts. *Phys. Rev. Lett.* **2015**, *115*, 261101. [CrossRef]
83. Wang, D.; Li, Z.; Zhang, J. Weak equivalence principle, swampland and $H_0$ tension with fast single radio bursts FRB 180924 and FRB 190523. *Phys. Dark Universe* **2020**, *29*, 100571. [CrossRef]
84. Gao, H.; Li, Z.; Zhang, B. Fast Radio Burst/Gamma-Ray Burst Cosmography. *Astrophys. J.* **2014**, *788*, 189. [CrossRef]
85. Zhou, B.; Li, X.; Wang, T.; Fan, Y.Z.; Wei, D.M. Fast radio bursts as a cosmic probe? *Phys. Rev. D* **2014**, *89*, 107303. [CrossRef]
86. Liu, B.; Li, Z.; Gao, H.; Zhu, Z.H. Prospects of strongly lensed repeating fast radio bursts: Complementary constraints on dark energy evolution. *Phys. Rev. D* **2019**, *99*, 123517. [CrossRef]
87. Ravi, V. The prevalence of repeating fast radio bursts. *Nat. Astron.* **2019**, *3*, 928–931. [CrossRef]
88. Prochaska, J.X.; Macquart, J.P.; McQuinn, M.; Simha, S.; Shannon, R.M.; Day, C.K.; Marnoch, L.; Ryder, S.; Deller, A.; Bannister, K.W.; et al. The low density and magnetization of a massive galaxy halo exposed by a fast radio burst. *Science* **2019**, *366*, 231–234. [CrossRef]
89. Macquart, J.P.; Prochaska, J.X.; McQuinn, M.; Bannister, K.W.; Bhandari, S.; Day, C.K.; Deller, A.T.; Ekers, R.D.; James, C.W.; Marnoch, L.; et al. A census of baryons in the Universe from localized fast radio bursts. *Nature* **2020**, *581*, 391–395. [CrossRef]
90. Wu, Q.; Yu, H.; Wang, F.Y. A New Method to Measure Hubble Parameter H(z) Using Fast Radio Bursts. *Astrophys. J.* **2020**, *895*, 33. [CrossRef]
91. Jaroszynski, M. Fast radio bursts and cosmological tests. *Mon. Not. R. Astron. Soc.* **2019**, *484*, 1637–1644. [CrossRef]
92. Li, Z.X.; Gao, H.; Ding, X.H.; Wang, G.J.; Zhang, B. Strongly lensed repeating fast radio bursts as precision probes of the universe. *Nat. Commun.* **2018**, *9*, 3833. [CrossRef] [PubMed]
93. Caleb, M.; Flynn, C.; Stappers, B.W. Constraining the era of helium reionization using fast radio bursts. *Mon. Not. R. Astron. Soc.* **2019**, *485*, 2281–2286. [CrossRef]
94. Linder, E.V. Detecting helium reionization with fast radio bursts. *Phys. Rev. D* **2020**, *101*, 103019. [CrossRef]
95. Bhattacharya, M.; Kumar, P.; Linder, E.V. Fast Radio Burst Dispersion Measure Distribution as a Probe of Helium Reionization. *arXiv* **2020**, arXiv:2010.14530.
96. Beniamini, P.; Kumar, P.; Ma, X.; Quataert, E. Exploring the epoch of hydrogen reionization using FRBs. *Mon. Not. R. Astron. Soc.* **2021**, *502*, 5134–5146. [CrossRef]
97. Madhavacheril, M.S.; Battaglia, N.; Smith, K.M.; Sievers, J.L. Cosmology with kSZ: Breaking the optical depth degeneracy with Fast Radio Bursts. *arXiv* **2019**, arXiv:1901.02418.
98. Connor, L.; van Leeuwen, J.; Oostrum, L.C.; Petroff, E.; Maan, Y.; Adams, E.A.K.; Attema, J.J.; Bast, J.E.; Boersma, O.M.; Dénes, H.; et al. A bright, high rotation-measure FRB that skewers the M33 halo. *Mon. Not. R. Astron. Soc.* **2020**, *499*, 4716–4724. [CrossRef]
99. Ravi, V.; Catha, M.; D'Addario, L.; Djorgovski, S.G.; Hallinan, G.; Hobbs, R.; Kocz, J.; Kulkarni, S.R.; Shi, J.; Vedantham, H.K.; et al. A fast radio burst localized to a massive galaxy. *Nature* **2019**, *572*, 352–354. [CrossRef] [PubMed]
100. Majid, W.A.; Pearlman, A.B.; Nimmo, K.; Hessels, J.W.T.; Prince, T.A.; Naudet, C.J.; Kocz, J.; Horiuchi, S. A Dual-band Radio Observation of FRB 121102 with the Deep Space Network and the Detection of Multiple Bursts. *Astrophys. J. Lett.* **2020**, *897*, L4. [CrossRef]
101. Hardy, L.K.; Dhillon, V.S.; Spitler, L.G.; Littlefair, S.P.; Ashley, R.P.; De Cia, A.; Green, M.J.; Jaroenjittichai, P.; Keane, E.F.; Kerry, P.; et al. A search for optical bursts from the repeating fast radio burst FRB 121102. *Mon. Not. R. Astron. Soc.* **2017**, *472*, 2800–2807. [CrossRef]
102. Hilmarsson, G.H.; Michilli, D.; Spitler, L.G.; Wharton, R.S.; Demorest, P.; Desvignes, G.; Gourdji, K.; Hackstein, S.; Hessels, J.W.T.; Nimmo, K.; et al. Rotation Measure Evolution of the Repeating Fast Radio Burst Source FRB 121102. *arXiv* **2020**, arXiv:2009.12135.
103. Luo, R.; Wang, B.J.; Men, Y.P.; Zhang, C.F.; Jiang, J.C.; Xu, H.; Wang, W.Y.; Lee, K.J.; Han, J.L.; Zhang, B.; et al. Diverse polarization angle swings from a repeating fast radio burst source. *Nature* **2020**, *586*, 693–696. [CrossRef]
104. Chawla, P.; Andersen, B.C.; Bhardwaj, M.; Fonseca, E.; Josephy, A.; Kaspi, V.M.; Michilli, D.; Pleunis, Z.; Bandura, K.M.; Bassa, C.G.; et al. Detection of Repeating FRB 180916.J0158+65 Down to Frequencies of 300 MHz. *Astrophys. J. Lett.* **2020**, *896*, L41. [CrossRef]
105. Marthi, V.R.; Gautam, T.; Li, D.Z.; Lin, H.H.; Main, R.A.; Naidu, A.; Pen, U.L.; Wharton, R.S. Detection of 15 bursts from the fast radio burst 180916.J0158+65 with the upgraded Giant Metrewave Radio Telescope. *Mon. Not. R. Astron. Soc.* **2020**, *499*, L16–L20. [CrossRef]
106. Pastor-Marazuela, I.; Connor, L.; van Leeuwen, J.; Maan, Y.; ter Veen, S.; Bilous, A.; Oostrum, L.; Petroff, E.; Straal, S.; Vohl, D.; et al. Chromatic periodic activity down to 120 MHz in a Fast Radio Burst. *arXiv* **2020**, arXiv:2012.08348.
107. Rajwade, K.M.; Mickaliger, M.B.; Stappers, B.W.; Morello, V.; Agarwal, D.; Bassa, C.G.; Breton, R.P.; Caleb, M.; Karastergiou, A.; Keane, E.F.; et al. Possible periodic activity in the repeating FRB 121102. *Mon. Not. R. Astron. Soc.* **2020**, *495*, 3551–3558. [CrossRef]
108. Jonas, J.; MeerKAT Team. The MeerKAT Radio Telescope. MeerKAT Science: On the Pathway to the SKA. 2016; p. 1. Available online: https://ui.adsabs.harvard.edu/abs/2016mks..confE...1J%2F/abstract (accessed on 8 May 2021).

109. Locatelli, N.T.; Bernardi, G.; Bianchi, G.; Chiello, R.; Magro, A.; Naldi, G.; Pilia, M.; Pupillo, G.; Ridolfi, A.; Setti, G.; et al. The Northern Cross fast radio burst project—I. Overview and pilot observations at 408 MHz. *Mon. Not. R. Astron. Soc.* **2020**, *494*, 1229–1236. [CrossRef]
110. Hobbs, G.; Manchester, R.N.; Dunning, A.; Jameson, A.; Roberts, P.; George, D.; Green, J.A.; Tuthill, J.; Toomey, L.; Kaczmarek, J.F.; et al. An ultra-wide bandwidth (704 to 4 032 MHz) receiver for the Parkes radio telescope. *Publ. Astron. Soc. Aust.* **2020**, *37*, e012. [CrossRef]
111. Prandoni, I.; Murgia, M.; Tarchi, A.; Burgay, M.; Castangia, P.; Egron, E.; Govoni, F.; Pellizzoni, A.; Ricci, R.; Righini, S.; et al. The Sardinia Radio Telescope. From a technological project to a radio observatory. *Astron. Astrophys.* **2017**, *608*, A40. [CrossRef]
112. Bailes, M.; Jameson, A.; Flynn, C.; Bateman, T.; Barr, E.D.; Bhandari, S.; Bunton, J.D.; Caleb, M.; Campbell-Wilson, D.; Farah, W.; et al. The UTMOST: A Hybrid Digital Signal Processor Transforms the Molonglo Observatory Synthesis Telescope. *Publ. Astron. Soc. Aust.* **2017**, *34*, e045. [CrossRef]
113. Law, C.J.; Bower, G.C.; Burke-Spolaor, S.; Butler, B.J.; Demorest, P.; Halle, A.; Khudikyan, S.; Lazio, T.J.W.; Pokorny, M.; Robnett, J.; et al. Realfast: Real-time, Commensal Fast Transient Surveys with the Very Large Array. *Astrophys. J. Suppl. Ser.* **2018**, *236*, 8. [CrossRef]
114. Coenen, T.; van Leeuwen, J.; Hessels, J.W.T.; Stappers, B.W.; Kondratiev, V.I.; Alexov, A.; Breton, R.P.; Bilous, A.; Cooper, S.; Falcke, H.; et al. The LOFAR pilot surveys for pulsars and fast radio transients. *Astron. Astrophys.* **2014**, *570*, A60. [CrossRef]
115. Karastergiou, A.; Chennamangalam, J.; Armour, W.; Williams, C.; Mort, B.; Dulwich, F.; Salvini, S.; Magro, A.; Roberts, S.; Serylak, M.; et al. Limits on fast radio bursts at 145 MHz with ARTEMIS, a real-time software backend. *Mon. Not. R. Astron. Soc.* **2015**, *452*, 1254–1262. [CrossRef]
116. Tingay, S.J.; Trott, C.M.; Wayth, R.B.; Bernardi, G.; Bowman, J.D.; Briggs, F.; Cappallo, R.J.; Deshpande, A.A.; Feng, L.; Gaensler, B.M.; et al. A Search for Fast Radio Bursts at Low Frequencies with Murchison Widefield Array High Time Resolution Imaging. *Astron. J.* **2015**, *150*, 199. [CrossRef]
117. Shannon, R.M.; Macquart, J.P.; Bannister, K.W.; Ekers, R.D.; James, C.W.; Osłowski, S.; Qiu, H.; Sammons, M.; Hotan, A.W.; Voronkov, M.A.; et al. The dispersion-brightness relation for fast radio bursts from a wide-field survey. *Nature* **2018**, *562*, 386–390. [CrossRef] [PubMed]
118. Petroff, E.; van Straten, W.; Johnston, S.; Bailes, M.; Barr, E.D.; Bates, S.D.; Bhat, N.D.R.; Burgay, M.; Burke-Spolaor, S.; Champion, D.; et al. An Absence of Fast Radio Bursts at Intermediate Galactic Latitudes. *Astrophys. J. Lett.* **2014**, *789*, L26. [CrossRef]
119. Macquart, J.P.; Johnston, S. On the paucity of fast radio bursts at low Galactic latitudes. *Mon. Not. R. Astron. Soc.* **2015**, *451*, 3278–3286. [CrossRef]
120. Bhandari, S.; Keane, E.F.; Barr, E.D.; Jameson, A.; Petroff, E.; Johnston, S.; Bailes, M.; Bhat, N.D.R.; Burgay, M.; Burke-Spolaor, S.; et al. The SUrvey for Pulsars and Extragalactic Radio Bursts II: New FRB discoveries and their follow-up. *Mon. Not. R. Astron. Soc.* **2018**, *475*, 1427–1446. [CrossRef]
121. Niu, C.H.; Li, D.; Luo, R.; Wang, W.Y.; Yao, J.; Zhang, B.; Zhu, W.W.; Wang, P.; Ye, H.; Zhang, Y.K.; et al. CRAFTS for Fast Radio Bursts Extending the dispersion-fluence relation with new FRBs detected by FAST. *arXiv* **2021**, arXiv:2102.10546.
122. The CHIME/FRB Collaboration; Amiri, M.; Andersen, B.C.; Bandura, K.; Berger, S.; Bhardwaj, M.; Boyce, M.M.; Boyle, P.J.; Brar, C.; Breitman, D.; et al. The First CHIME/FRB Fast Radio Burst Catalog. *arXiv* **2021**, arXiv:2106.04352.
123. Rafiei-Ravandi, M.; Smith, K.M.; Li, D.; Masui, K.W.; Josephy, A.; Dobbs, M.; Lang, D.; Bhardwaj, M.; Patel, C.; Bandura, K.; et al. CHIME/FRB Catalog 1 results: Statistical cross-correlations with large-scale structure. *arXiv* **2021**, arXiv:2106.04354.
124. Chime/Frb Collaboration; Amiri, M.; Andersen, B.C.; Bandura, K.M.; Bhardwaj, M.; Boyle, P.J.; Brar, C.; Chawla, P.; Chen, T.; Cliche, J.F.; et al. Periodic activity from a fast radio burst source. *Nature* **2020**, *582*, 351–355. [CrossRef]
125. Aggarwal, K.; Law, C.J.; Burke-Spolaor, S.; Bower, G.; Butler, B.J.; Demorest, P.; Linford, J.; Lazio, T.J.W. VLA/Realfast Detection of a Burst from FRB 180916.J0158+65 and Tests for Periodic Activity. *Res. Notes Am. Astron. Soc.* **2020**, *4*, 94. [CrossRef]
126. Cruces, M.; Spitler, L.G.; Scholz, P.; Lynch, R.; Seymour, A.; Hessels, J.W.T.; Gouiffés, C.; Hilmarsson, G.H.; Kramer, M.; Munjal, S. Repeating behaviour of FRB 121102: Periodicity, waiting times, and energy distribution. *Mon. Not. R. Astron. Soc.* **2021**, *500*, 448–463. [CrossRef]
127. Ioka, K.; Zhang, B. A Binary Comb Model for Periodic Fast Radio Bursts. *Astrophys. J. Lett.* **2020**, *893*, L26. [CrossRef]
128. Sridhar, N.; Metzger, B.D.; Beniamini, P.; Margalit, B.; Renzo, M.; Sironi, L.; Kovlakas, K. Periodic Fast Radio Bursts from Luminous X-ray Binaries. *Astrophys. J.* **2021**, *917*, 13. [CrossRef]
129. Zanazzi, J.J.; Lai, D. Periodic Fast Radio Bursts with Neutron Star Free Precession. *Astrophys. J. Lett.* **2020**, *892*, L15. [CrossRef]
130. Tong, H.; Wang, W.; Wang, H.G. Periodicity in fast radio bursts due to forced precession by a fallback disk. *Res. Astron. Astrophys.* **2020**, *20*, 142. [CrossRef]
131. Li, D.; Wang, P.; Zhu, W.W.; Zhang, B.; Zhang, X.X.; Duan, R.; Zhang, Y.K.; Feng, Y.; Tang, N.Y.; Chatterjee, S.; et al. A bimodal burst energy distribution of a repeating fast radio burst source. *arXiv* **2021**, arXiv:2107.08205.
132. Caleb, M.; Stappers, B.W.; Rajwade, K.; Flynn, C. Are all fast radio bursts repeating sources? *Mon. Not. R. Astron. Soc.* **2019**, *484*, 5500–5508. [CrossRef]
133. Patek, C.; Chime/Frb Collaboration. CHIME/FRB Detection of a Repeat Burst from ASKAP-Discovered FRB 171019. *Astron. Telegr.* **2019**, *13013*, 1.
134. James, C.W. Limits on the population of repeating fast radio bursts from the ASKAP/CRAFT lat50 survey. *Mon. Not. R. Astron. Soc.* **2019**, *486*, 5934–5950. [CrossRef]

135. Oppermann, N.; Yu, H.R.; Pen, U.L. On the non-Poissonian repetition pattern of FRB121102. *Mon. Not. R. Astron. Soc.* **2018**, *475*, 5109–5115. [CrossRef]
136. Caleb, M.; Stappers, B.W.; Abbott, T.D.; Barr, E.D.; Bezuidenhout, M.C.; Buchner, S.J.; Burgay, M.; Chen, W.; Cognard, I.; Driessen, L.N.; et al. Simultaneous multi-telescope observations of FRB 121102. *Mon. Not. R. Astron. Soc.* **2020**, *496*, 4565–4573. [CrossRef]
137. Scholz, P.; Bogdanov, S.; Hessels, J.W.T.; Lynch, R.S.; Spitler, L.G.; Bassa, C.G.; Bower, G.C.; Burke-Spolaor, S.; Butler, B.J.; Chatterjee, S.; et al. Simultaneous X-Ray, Gamma-Ray, and Radio Observations of the Repeating Fast Radio Burst FRB 121102. *Astrophys. J.* **2017**, *846*, 80. [CrossRef]
138. Gourdji, K.; Michilli, D.; Spitler, L.G.; Hessels, J.W.T.; Seymour, A.; Cordes, J.M.; Chatterjee, S. A Sample of Low-energy Bursts from FRB 121102. *Astrophys. J. Lett.* **2019**, *877*, L19. [CrossRef]
139. Cho, H.; Macquart, J.P.; Shannon, R.M.; Deller, A.T.; Morrison, I.S.; Ekers, R.D.; Bannister, K.W.; Farah, W.; Qiu, H.; Sammons, M.W.; et al. Spectropolarimetric Analysis of FRB 181112 at Microsecond Resolution: Implications for Fast Radio Burst Emission Mechanism. *Astrophys. J. Lett.* **2020**, *891*, L38. [CrossRef]
140. Farah, W.; Flynn, C.; Bailes, M.; Jameson, A.; Bannister, K.W.; Barr, E.D.; Bateman, T.; Bhandari, S.; Caleb, M.; Campbell-Wilson, D.; et al. FRB microstructure revealed by the real-time detection of FRB170827. *Mon. Not. R. Astron. Soc.* **2018**, *478*, 1209–1217. [CrossRef]
141. Luo, R.; Lee, K.; Lorimer, D.R.; Zhang, B. On the normalized FRB luminosity function. *Mon. Not. R. Astron. Soc.* **2018**, *481*, 2320–2337. [CrossRef]
142. Lu, W.; Kumar, P.; Zhang, B. A unified picture of Galactic and cosmological fast radio bursts. *Mon. Not. R. Astron. Soc.* **2020**, *498*, 1397–1405. [CrossRef]
143. Ghisellini, G.; Locatelli, N. Coherent curvature radiation and fast radio bursts. *Astron. Astrophys.* **2018**, *613*, A61. [CrossRef]
144. Yang, Y.P.; Zhang, B. Bunching Coherent Curvature Radiation in Three-dimensional Magnetic Field Geometry: Application to Pulsars and Fast Radio Bursts. *Astrophys. J.* **2018**, *868*, 31. [CrossRef]
145. Lyubarsky, Y. Fast Radio Bursts from Reconnection in a Magnetar Magnetosphere. *Astrophys. J.* **2020**, *897*, 1. [CrossRef]
146. Metzger, B.D.; Margalit, B.; Sironi, L. Fast radio bursts as synchrotron maser emission from decelerating relativistic blast waves. *Mon. Not. R. Astron. Soc.* **2019**, *485*, 4091–4106. [CrossRef]
147. Wadiasingh, Z.; Chirenti, C. Fast Radio Burst Trains from Magnetar Oscillations. *Astrophys. J. Lett.* **2020**, *903*, L38. [CrossRef]
148. Ofek, E.O. Soft Gamma-Ray Repeaters in Nearby Galaxies: Rate, Luminosity Function, and Fraction among Short Gamma-Ray Bursts. *Astrophys. J.* **2007**, *659*, 339–346. [CrossRef]
149. Li, W.; Chornock, R.; Leaman, J.; Filippenko, A.V.; Poznanski, D.; Wang, X.; Ganeshalingam, M.; Mannucci, F. Nearby supernova rates from the Lick Observatory Supernova Search—III. The rate-size relation, and the rates as a function of galaxy Hubble type and colour. *Mon. Not. R. Astron. Soc.* **2011**, *412*, 1473–1507. [CrossRef]
150. Totani, T. Cosmological Fast Radio Bursts from Binary Neutron Star Mergers. *Publ. Astron. Soc. Jpn.* **2013**, *65*, L12. [CrossRef]
151. Kashiyama, K.; Ioka, K.; Mészáros, P. Cosmological Fast Radio Bursts from Binary White Dwarf Mergers. *Astrophys. J. Lett.* **2013**, *776*, L39. [CrossRef]
152. Yamasaki, S.; Totani, T.; Kiuchi, K. Repeating and non-repeating fast radio bursts from binary neutron star mergers. *Publ. Astron. Soc. Jpn.* **2018**, *70*, 39. [CrossRef]
153. Popov, S.B.; Postnov, K.A. Hyperflares of SGRs as an engine for millisecond extragalactic radio bursts. In *Evolution of Cosmic Objects through Their Physical Activity, Proceedings of the Conference Dedicated to Viktor Ambartsumian's 100th Anniversary, Yerevan, Armenia, 15–18 September 2008*; Harutyunian, H.A., Mickaelian, A.M., Terzian, Y., Eds.; Gitutyun Publishing House: Yerevan, Armenia, 2010; pp. 129–132.
154. Cordes, J.M.; Wasserman, I. Supergiant pulses from extragalactic neutron stars. *Mon. Not. R. Astron. Soc.* **2016**, *457*, 232–257. [CrossRef]
155. Vedantham, H.K.; Ravi, V.; Hallinan, G.; Shannon, R.M. The Fluence and Distance Distributions of Fast Radio Bursts. *Astrophys. J.* **2016**, *830*, 75. [CrossRef]
156. Macquart, J.P.; Ekers, R. FRB event rate counts—II. Fluence, redshift, and dispersion measure distributions. *Mon. Not. R. Astron. Soc.* **2018**, *480*, 4211–4230. [CrossRef]
157. James, C.W.; Prochaska, J.X.; Macquart, J.P.; North-Hickey, F.; Bannister, K.W.; Dunning, A. The fast radio burst population evolves, consistent with the star-formation rate. *arXiv* **2021**, arXiv:2101.07998.
158. Williamson, I.P. Pulse broadening due to multiple scattering in the interstellarmedium-II. *Mon. Not. R. Astron. Soc.* **1973**, *163*, 345. [CrossRef]
159. Williamson, I.P. Pulse broadening due to multiple scattering in the interstellarmedium. *Mon. Not. R. Astron. Soc.* **1972**, *157*, 55. [CrossRef]
160. Qiu, H.; Shannon, R.M.; Farah, W.; Macquart, J.P.; Deller, A.T.; Bannister, K.W.; James, C.W.; Flynn, C.; Day, C.K.; Bhandari, S.; et al. A population analysis of pulse broadening in ASKAP fast radio bursts. *Mon. Not. R. Astron. Soc.* **2020**, *497*, 1382–1390. [CrossRef]
161. Bhat, N.D.R.; Cordes, J.M.; Camilo, F.; Nice, D.J.; Lorimer, D.R. Multifrequency Observations of Radio Pulse Broadening and Constraints on Interstellar Electron Density Microstructure. *Astrophys. J.* **2004**, *605*, 759–783. [CrossRef]

162. Chawla, P.; Kaspi, V.M.; Ransom, S.M.; Bhardwaj, M.; Boyle, P.J.; Breitman, D.; Cassanelli, T.; Cubranic, D.; Dong, F.Q.; Fonseca, E.; et al. Modeling Fast Radio Burst Dispersion and Scattering Properties in the First CHIME/FRB Catalog. *arXiv* **2021**, arXiv:2107.10858.
163. Hessels, J.W.T.; Spitler, L.G.; Seymour, A.D.; Cordes, J.M.; Michilli, D.; Lynch, R.S.; Gourdji, K.; Archibald, A.M.; Bassa, C.G.; Bower, G.C.; et al. FRB 121102 Bursts Show Complex Time-Frequency Structure. *Astrophys. J. Lett.* **2019**, *876*, L23. [CrossRef]
164. Ravi, V.; Shannon, R.M.; Bailes, M.; Bannister, K.; Bhandari, S.; Bhat, N.D.R.; Burke-Spolaor, S.; Caleb, M.; Flynn, C.; Jameson, A.; et al. The magnetic field and turbulence of the cosmic web measured using a brilliant fast radio burst. *Science* **2016**, *354*, 1249–1252. [CrossRef]
165. Michilli, D.; Seymour, A.; Hessels, J.W.T.; Spitler, L.G.; Gajjar, V.; Archibald, A.M.; Bower, G.C.; Chatterjee, S.; Cordes, J.M.; Gourdji, K.; et al. An extreme magneto-ionic environment associated with the fast radio burst source FRB 121102. *Nature* **2018**, *553*, 182–185. [CrossRef] [PubMed]
166. Wang, W.; Zhang, B.; Chen, X.; Xu, R. On the Time-Frequency Downward Drifting of Repeating Fast Radio Bursts. *Astrophys. J. Lett.* **2019**, *876*, L15. [CrossRef]
167. Josephy, A.; Chawla, P.; Fonseca, E.; Ng, C.; Patel, C.; Pleunis, Z.; Scholz, P.; Andersen, B.C.; Bandura, K.; Bhardwaj, M.; et al. CHIME/FRB Detection of the Original Repeating Fast Radio Burst Source FRB 121102. *Astrophys. J. Lett.* **2019**, *882*, L18. [CrossRef]
168. Chamma, M.A.; Rajabi, F.; Wyenberg, C.M.; Mathews, A.; Houde, M. Evidence of a shared spectro-temporal law between sources of repeating fast radio bursts. *Mon. Not. R. Astron. Soc.* **2021**, *507*, 246–260. [CrossRef]
169. Cordes, J.M.; Wasserman, I.; Hessels, J.W.T.; Lazio, T.J.W.; Chatterjee, S.; Wharton, R.S. Lensing of Fast Radio Bursts by Plasma Structures in Host Galaxies. *Astrophys. J.* **2017**, *842*, 35. [CrossRef]
170. Platts, E.; Caleb, M.; Stappers, B.W.; Main, R.A.; Weltman, A.; Shock, J.P.; Kramer, M.; Bezuidenhout, M.C.; Jankowski, F.; Morello, V.; et al. An analysis of the time-frequency structure of several bursts from FRB 121102 detected with MeerKAT. *Mon. Not. R. Astron. Soc.* **2021**, *505*, 3041–3053. [CrossRef]
171. Vedantham, H.K.; Ravi, V. Faraday conversion and magneto-ionic variations in fast radio bursts. *Mon. Not. R. Astron. Soc.* **2019**, *485*, L78–L82. [CrossRef]
172. Gruzinov, A.; Levin, Y. Conversion Measure of Faraday Rotation-Conversion with Application to Fast Radio Bursts. *Astrophys. J.* **2019**, *876*, 74. [CrossRef]
173. Zhang, B. FRB 121102: A Repeatedly Combed Neutron Star by a Nearby Low-luminosity Accreting Supermassive Black Hole. *Astrophys. J. Lett.* **2018**, *854*, L21. [CrossRef]
174. Wang, W.Y.; Zhang, B.; Chen, X.; Xu, R. On the magnetoionic environments of fast radio bursts. *Mon. Not. R. Astron. Soc.* **2020**, *499*, 355–361. [CrossRef]
175. Lu, W.; Kumar, P. On the radiation mechanism of repeating fast radio bursts. *Mon. Not. R. Astron. Soc.* **2018**, *477*, 2470–2493. [CrossRef]
176. Petroff, E.; Burke-Spolaor, S.; Keane, E.F.; McLaughlin, M.A.; Miller, R.; Andreoni, I.; Bailes, M.; Barr, E.D.; Bernard, S.R.; Bhandari, S.; et al. A polarized fast radio burst at low Galactic latitude. *Mon. Not. R. Astron. Soc.* **2017**, *469*, 4465–4482. [CrossRef]
177. Keane, E.F.; Johnston, S.; Bhandari, S.; Barr, E.; Bhat, N.D.R.; Burgay, M.; Caleb, M.; Flynn, C.; Jameson, A.; Kramer, M.; et al. The host galaxy of a fast radio burst. *Nature* **2016**, *530*, 453–456. [CrossRef]
178. Caleb, M.; Keane, E.F.; van Straten, W.; Kramer, M.; Macquart, J.P.; Bailes, M.; Barr, E.D.; Bhat, N.D.R.; Bhandari, S.; Burgay, M.; et al. The SUrvey for Pulsars and Extragalactic Radio Bursts—III. Polarization properties of FRBs 160102 and 151230. *Mon. Not. R. Astron. Soc.* **2018**, *478*, 2046–2055. [CrossRef]
179. Osłowski, S.; Shannon, R.M.; Ravi, V.; Kaczmarek, J.F.; Zhang, S.; Hobbs, G.; Bailes, M.; Russell, C.J.; van Straten, W.; James, C.W.; et al. Commensal discovery of four fast radio bursts during Parkes Pulsar Timing Array observations. *Mon. Not. R. Astron. Soc.* **2019**, *488*, 868–875. [CrossRef]
180. Hilmarsson, G.H.; Spitler, L.G.; Main, R.A.; Li, D.Z. Polarization properties of FRB 20201124A from detections with the 100-m Effelsberg Radio Telescope. *arXiv* **2021**, arXiv:2107.12892.
181. Kramer, M.; Stappers, B.W.; Jessner, A.; Lyne, A.G.; Jordan, C.A. Polarized radio emission from a magnetar. *Mon. Not. R. Astron. Soc.* **2007**, *377*, 107–119. [CrossRef]
182. Jessner, A.; Popov, M.V.; Kondratiev, V.I.; Kovalev, Y.Y.; Graham, D.; Zensus, A.; Soglasnov, V.A.; Bilous, A.V.; Moshkina, O.A. Giant pulses with nanosecond time resolution detected from the Crab pulsar at 8.5 and 15.1 GHz. *Astron. Astrophys.* **2010**, *524*, A60. [CrossRef]
183. Scholz, P.; Spitler, L.G.; Hessels, J.W.T.; Chatterjee, S.; Cordes, J.M.; Kaspi, V.M.; Wharton, R.S.; Bassa, C.G.; Bogdanov, S.; Camilo, F.; et al. The Repeating Fast Radio Burst FRB 121102: Multi-wavelength Observations and Additional Bursts. *Astrophys. J.* **2016**, *833*, 177. [CrossRef]
184. Pleunis, Z.; Good, D.C.; Kaspi, V.M.; Mckinven, R.; Ransom, S.M.; Scholz, P.; Bandura, K.; Bhardwaj, M.; Boyle, P.J.; Brar, C.; et al. Fast Radio Burst Morphology in the First CHIME/FRB Catalog. *arXiv* **2021**, arXiv:2106.04356.
185. Margalit, B.; Metzger, B.D. A Concordance Picture of FRB 121102 as a Flaring Magnetar Embedded in a Magnetized Ion-Electron Wind Nebula. *Astrophys. J. Lett.* **2018**, *868*, L4. [CrossRef]
186. Waxman, E. On the Origin of Fast Radio Bursts (FRBs). *Astrophys. J.* **2017**, *842*, 34. [CrossRef]
187. Marcote, B.; Nimmo, K.; Hessels, J.W.T.; Tendulkar, S.P.; Bassa, C.G.; Paragi, Z.; Keimpema, A.; Bhardwaj, M.; Karuppusamy, R.; Kaspi, V.M.; et al. A repeating fast radio burst source localized to a nearby spiral galaxy. *Nature* **2020**, *577*, 190–194. [CrossRef]

188. Tendulkar, S.P.; Gil de Paz, A.; Kirichenko, A.Y.; Hessels, J.W.T.; Bhardwaj, M.; Ávila, F.; Bassa, C.; Chawla, P.; Fonseca, E.; Kaspi, V.M.; et al. The 60-pc Environment of FRB 20180916B. *arXiv* **2020**, arXiv:2011.03257.
189. Kirsten, F.; Marcote, B.; Nimmo, K.; Hessels, J.W.T.; Bhardwaj, M.; Tendulkar, S.P.; Keimpema, A.; Yang, J.; Snelders, M.P.; Scholz, P.; et al. A repeating fast radio burst source in a globular cluster. *arXiv* **2021**, arXiv:2105.11445.
190. Fong, W.F.; Dong, Y.; Leja, J.; Bhandari, S.; Day, C.K.; Deller, A.T.; Kumar, P.; Prochaska, J.X.; Scott, D.R.; Bannister, K.W.; et al. Chronicling the Host Galaxy Properties of the Remarkable Repeating FRB 20201124A. *arXiv* **2021**, arXiv:2106.11993.
191. Wharton, R.; Bethapudi, S.; Gautam, T.; Li, D.; Lin, H.H.; Main, R.; Marthi, V.; Spitler, L.; Pen, U.L. uGMRT detection of a persistent radio source coincident with FRB20201124A. *Astron. Telegr.* **2021**, *14529*, 1.
192. Ricci, R.; Piro, L.; Panessa, F.; O'Connor, B.; Lotti, S.; Bruni, G.; Zhang, B. Detection of a persistent radio source at the location of FRB20201124A with VLA. *Astron. Telegr.* **2021**, *14549*, 1.
193. Marcote, B.; Kirsten, F.; Hessels, J.W.T.; Nimmo, K.; Keimpema, A.; Paragi, Z.; Bach, U.; Burgay, M.; Corongiu, A.; Feiler, R.; et al. VLBI localization of FRB 20201124A and absence of persistent emission on milliarcsecond scales. *Astron. Telegr.* **2021**, *14603*, 1.
194. Heintz, K.E.; Prochaska, J.X.; Simha, S.; Platts, E.; Fong, W.F.; Tejos, N.; Ryder, S.D.; Aggerwal, K.; Bhandari, S.; Day, C.K.; et al. Host Galaxy Properties and Offset Distributions of Fast Radio Bursts: Implications for Their Progenitors. *Astrophys. J.* **2020**, *903*, 152. [CrossRef]
195. Law, C.J.; Butler, B.J.; Prochaska, J.X.; Zackay, B.; Burke-Spolaor, S.; Mannings, A.; Tejos, N.; Josephy, A.; Andersen, B.; Chawla, P.; et al. A Distant Fast Radio Burst Associated with Its Host Galaxy by the Very Large Array. *Astrophys. J.* **2020**, *899*, 161. [CrossRef]
196. Bannister, K.W.; Deller, A.T.; Phillips, C.; Macquart, J.P.; Prochaska, J.X.; Tejos, N.; Ryder, S.D.; Sadler, E.M.; Shannon, R.M.; Simha, S.; et al. A single fast radio burst localized to a massive galaxy at cosmological distance. *Science* **2019**, *365*, 565–570. [CrossRef]
197. Chittidi, J.S.; Simha, S.; Mannings, A.; Prochaska, J.X.; Rafelski, M.; Neeleman, M.; Macquart, J.P.; Tejos, N.; Jorgenson, R.A.; Ryder, S.D.; et al. Dissecting the Local Environment of FRB 190608 in the Spiral Arm of its Host Galaxy. *arXiv* **2020**, arXiv:2005.13158.
198. Bhandari, S.; Heintz, K.E.; Aggarwal, K.; Marnoch, L.; Day, C.K.; Sydnor, J.; Burke-Spolaor, S.; Law, C.J.; Prochaska, J.X.; Tejos, N.; et al. Characterizing the FRB host galaxy population and its connection to transients in the local and extragalactic Universe. *arXiv* **2021**, arXiv:2108.01282.
199. Li, Y.; Zhang, B. A Comparative Study of Host Galaxy Properties between Fast Radio Bursts and Stellar Transients. *Astrophys. J. Lett.* **2020**, *899*, L6. [CrossRef]
200. Mannings, A.G.; Fong, W.F.; Simha, S.; Prochaska, J.X.; Rafelski, M.; Kilpatrick, C.D.; Tejos, N.; Heintz, K.E.; Bhandari, S.; Day, C.K.; et al. A High-Resolution View of Fast Radio Burst Host Environments. *arXiv* **2020**, arXiv:2012.11617.
201. Safarzadeh, M.; Prochaska, J.X.; Heintz, K.E.; Fong, W.f. Confronting the Magnetar Interpretation of Fast Radio Bursts through Their Host Galaxy Demographics. *Astrophys. J. Lett.* **2020**, *905*, L30. [CrossRef]
202. Baldwin, J.A.; Phillips, M.M.; Terlevich, R. Classification parameters for the emission-line spectra of extragalactic objects. *Publ. Astron. Soc. Pac.* **1981**, *93*, 5–19. [CrossRef]
203. Bailes, M.; Bassa, C.G.; Bernardi, G.; Buchner, S.; Burgay, M.; Caleb, M.; Cooper, A.J.; Desvignes, G.; Groot, P.J.; Heywood, I.; et al. Multifrequency observations of SGR J1935+2154. *Mon. Not. R. Astron. Soc.* **2021**, *503*, 5367–5384. [CrossRef]
204. Bhandari, S.; Sadler, E.M.; Prochaska, J.X.; Simha, S.; Ryder, S.D.; Marnoch, L.; Bannister, K.W.; Macquart, J.P.; Flynn, C.; Shannon, R.M.; et al. The Host Galaxies and Progenitors of Fast Radio Bursts Localized with the Australian Square Kilometre Array Pathfinder. *Astrophys. J. Lett.* **2020**, *895*, L37. [CrossRef]
205. Keane, E.F.; Petroff, E. Fast radio bursts: Search sensitivities and completeness. *Mon. Not. R. Astron. Soc.* **2015**, *447*, 2852–2856. [CrossRef]
206. Connor, L. Interpreting the distributions of FRB observables. *Mon. Not. R. Astron. Soc.* **2019**, *487*, 5753–5763. [CrossRef]
207. Zhang, B. Fast Radio Bursts from Interacting Binary Neutron Star Systems. *Astrophys. J. Lett.* **2020**, *890*, L24. [CrossRef]
208. Margalit, B.; Berger, E.; Metzger, B.D. Fast Radio Bursts from Magnetars Born in Binary Neutron Star Mergers and Accretion Induced Collapse. *Astrophys. J.* **2019**, *886*, 110. [CrossRef]
209. Wang, F.Y.; Wang, Y.Y.; Yang, Y.P.; Yu, Y.W.; Zuo, Z.Y.; Dai, Z.G. Fast Radio Bursts from Activity of Neutron Stars Newborn in BNS Mergers: Offset, Birth Rate, and Observational Properties. *Astrophys. J.* **2020**, *891*, 72. [CrossRef]
210. Metzger, B.D.; Fang, K.; Margalit, B. Neutrino Counterparts of Fast Radio Bursts. *Astrophys. J. Lett.* **2020**, *902*, L22. [CrossRef]